Stapled Peptides Inhibitors

Ali, Ameena M.; Atmaj, Jack; Van Oosterwijk, Niels; Groves, Matthew R.; Dömling, Alexander

Published in:
Computational and Structural Biotechnology Journal

DOI:
10.1016/j.csbj.2019.01.012

Publication date:
2019

Computational and Structural Biotechnology Journal 17 (2019) 263–281

COMPUTATIONAL AND STRUCTURAL BIOTECHNOLOGY JOURNAL

journal homepage: www.elsevier.com/locate/csbj

Mini Review

Stapled Peptides Inhibitors: A New Window for Target Drug Discovery

Ameena M. Ali, Jack Atmaj, Niels Van Oosterwijk, Matthew R. Groves, Alexander Dömling *

Department of Drug Design, University of Groningen, Antonius Deusinglaan1, 9700AD Groningen, the Netherlands

ARTICLE INFO

Article history:
Received 22 November 2018
Received in revised form 28 January 2019
Accepted 29 January 2019
Available online 19 February 2019

Keywords:
Stapled peptide
PPI
Drug discovery
Inhibitor
Synthetic chemistry

ABSTRACT

Protein-protein interaction (PPI) is a hot topic in clinical research as protein networking has a major impact in human disease. Such PPIs are potential drugs targets, leading to the need to inhibit/block specific PPIs. While small molecule inhibitors have had some success and reached clinical trials, they have generally failed to address the flat and large nature of PPI surfaces. As a result, larger biologics were developed for PPI surfaces and they have successfully targeted PPIs located outside the cell. However, biologics have low bioavailability and cannot reach intracellular targets. A novel class -hydrocarbon-stapled α-helical peptides that are synthetic mini-proteins locked into their bioactive structure through site-specific introduction of a chemical linker- has shown promise. Stapled peptides show an ability to inhibit intracellular PPIs that previously have been intractable with traditional small molecule or biologics, suggesting that they offer a novel therapeutic modality. In this review, we highlight what stapling adds to natural-mimicking peptides, describe the revolution of synthetic chemistry techniques and how current drug discovery approaches have been adapted to stabilize active peptide conformations, including ring-closing metathesis (RCM), lactamisation, cycloadditions and reversible reactions. We provide an overview on the available stapled peptide high-resolution structures in the protein data bank, with four selected structures discussed in details due to remarkable interactions of their staple with the target surface. We believe that stapled peptides are promising drug candidates and open the doors for peptide therapeutics to reach currently "undruggable" space.

Contents

* Corresponding author.
E-mail address: a.s.s.domling@rug.nl (A. Dömling).

https://doi.org/10.1016/j.csbj.2019.01.012

1. Introduction

Drug discovery approaches targeting protein-protein interactions (PPIs) has been fast-tracked over the present decade to deliver successful new drug leads and opens an expansive range of new therapeutic targets that were previously considered "undruggable". This acceleration in PPI-based drugs is due to improved screening and design technologies, shortening the time between drug discovery to drug registration and changing pharmaceutical economic delivery [1]. Moreover, most human diseases are underpinned by a complex network of PPIs, (for example hubs such as p53), which underscores the need to understand PPIs not only on a clinical level, but also on molecular level. In this respect, the "omics" such as, genomics, RNA, proteomics and metabolomics can accumulate huge volumes of data aiming at targeted and personalized medicine [2,3].

All of the data, in addition to structural and screening-based approaches, have significantly expanded our understanding on PPI interfaces that were previously highly challenging and difficult to target, as these interacting surfaces are shallow or flat, non-hydrophobic and large (1500-3000 Å). In addition, PPI surfaces differ in their shape and amino acid residue composition, particularly the hot spots that are essential during binding protein partners; making small-molecules entities unlikely as protein therapeutics [4–8]. Moreover, the discovery of innovative and drug lead molecules with the expected biological activity and pharmacokinetics is the main aim of medicinal chemistry. Therefore, the application of 'follow-on'-based strategy has always been one of the most effective approaches that lead to promising bioactive molecules. Conformational restrictions or "rigidification" is one of these strategies that has been widely used to overcome ligand flexibility, which suffer from entropic penalty upon binding to the target surface [9]. The restriction strategy has two major advantages: firstly, it could increase the potency of the drug-like agent by stabilizing a favorable binding conformation, reducing the entropic penalty on binding to the target and decrease its degradation by hindering metabolically labile sites or introducing a fused-ring structure; in addition to improve isoform selectivity or specificity toward targets. Secondly, controlling ligand confirmation could improve affinity on the atomic level without requiring additional interactions [9,10].

There are two types of drugs generally available on the market: traditional small-molecule drugs with molecular weight of <500 Da and high oral bioavailability but low target selectivity; and biologics that are typically >5000 Da (such as insulin, growth factors, erythropoietin (EPO) and engineered antibodies) that have limited oral bioavailability, poor membrane permeability and metabolic instability. As a result such medications are typically delivered by injection. However, biologics have extremely high specificity and affinity for their targets due to the large area of interaction with their targets [1,11]. Despite the success of both drug classes in treating different diseases, there remains an opportunity to offer a class of molecules to fill the gap in molecular weight between the existing two classes (Small molecules <500…Peptides…Biologics >5000 Da) and merge some of the advantages of small-molecules and biologics in terms of oral bioavailability, cell penetration and cheaper manufacturing costs. This class could be considered to be a next generation therapeutic class that precisely targets PPIs and is based upon hydrocarbon-stapled α-helical peptides. Fig. 1 represents the three classes of targeted drugs based on their molecular weight.

In this review we will focus on hydrocarbon-stapled α-helical peptides and their use as potential drugs. Hydrocarbon α-helical peptides are synthetic mini-proteins locked into their bioactive α-helix secondary structure by site-specific insertion of a synthetic chemical staple linker or "brace". Stapled peptides show a greatly improved pharmacologic performance, increased affinity to their target, resistance to proteolytic digestion, and afford high levels of cell penetration via endocytic vesicle trafficking [5,12–14].

In this review we will discuss what stapling adds to this class of inhibitors in terms of stability, bioactivity and cell penetration, the chemistry behind peptide stapling and provide an overview on some selected successful examples of peptide-based drugs to underline their importance. Lastly, we will underline four exclusive stapled-peptides targeting PPIs, in which their staple makes an intimate interaction with the target interface, in order to reveal the role of stapling on peptide binding and their inhibition of PPIs.

2. Why Stapled Peptides?

Helical peptides are one of the two main secondary structural elements in PPI interfaces, (in addition to β-sheets) and play a central role in protein function within the cell. Often these elements are not stable in conformation in the absence of a complete protein fold. Additionally, peptides are sensitive to proteolysis by peptidases reducing their half-life (down to minutes), impacting their ability to penetrate cell membranes – all of which makes native peptides poor drug candidates [14–16]. Notwithstanding, one main feature that makes peptides good drug candidates is their ability to bind large and relatively flat target surfaces efficiently and specifically, which is a requirement in the majority of intracellular therapeutically relevant PPIs. This makes peptides as an attractive target for drug development and enables their transition into the clinic [5,17]. The use of therapeutic peptides has grown explosively over the last three decades, covering areas such as metabolic diseases, oncology, and cardiovascular diseases [18]. From a dataset that was collected recently on March 2018 and based on previously released database report by Peptide Therapeutics Foundation, of 484 therapeutic peptides, 60 have been approved in the United States, Europe, and/or Japan, 155 peptides are in clinical development and 50% are currently in Phase II studies (Fig. 2) [18].

Massive efforts and optimizations have been conducted in order to overcome the limitations above. To impose a peptide α-helix conformation (thereby improving their binding affinity toward their target protein) non-native amino acids were used in the peptide that lie on the same helix face. These non native amino acids are then linked together or "stapled" through side-chains that can be covalently bonded [16,19].

In order to address a second issue, to synthesize peptides with resistance toward proteases, non-peptide (such as cyclic tripeptides, heterocyclic or other organic constraints) are inserted into a peptide sequence to maintain the peptide backbone in a linear saw-toothed strand structure [20–23]. These chemical modifications have evolved over time since the first all-hydrocarbon stapling by Verdine and colleagues in 2000, who produced a large series of α, α-disubstituted non-natural amino acids bearing olefin tethers (Fig. 3a). His work was an extension of Blackwell and Grubbs, who were the first to use Grubbs catalysts to make a cross-link between O-allylserine residues on a peptide template (Fig. 3b). Walensky provided the bridge between chemistry and biology by generating hydrocarbon- stapled BH3 peptide helices, targeting BCL-2 homology 3 domains responsible for the interactions of BCL-2 family proteins that mainly regulate cellular life and death at the mitochondrial level. This stapled peptide not only showed a higher stability and remarkable resistance to proteolysis, but also high cellular permeability [19,24,25]. The details of stapled-peptide chemical synthesis will be discussed in detail in Section 3.

Interestingly, peptides could be differentiated from proteins by their size (50 amino acids or less) but have similar specificity toward their targets as biologics. However, peptides are more potent binders to PPIs interfaces, because of their ability to bind large protein surfaces with great selectivity and less toxicity when compared to small molecule drugs, which often produce toxic metabolites. In contrast to small molecules, peptides are degraded into amino acids, which are in turn not toxic or harmful for cells [1,26]. Furthermore, peptides have lower manufacturing costs and are more stable at room temperature (unlike recombinant antibodies and engineered proteins). Finally, as non-natural amino acids are the building blocks of peptides, the opportunity to produce diverse scaffolds with modified chemical and functional properties is available [27,28].

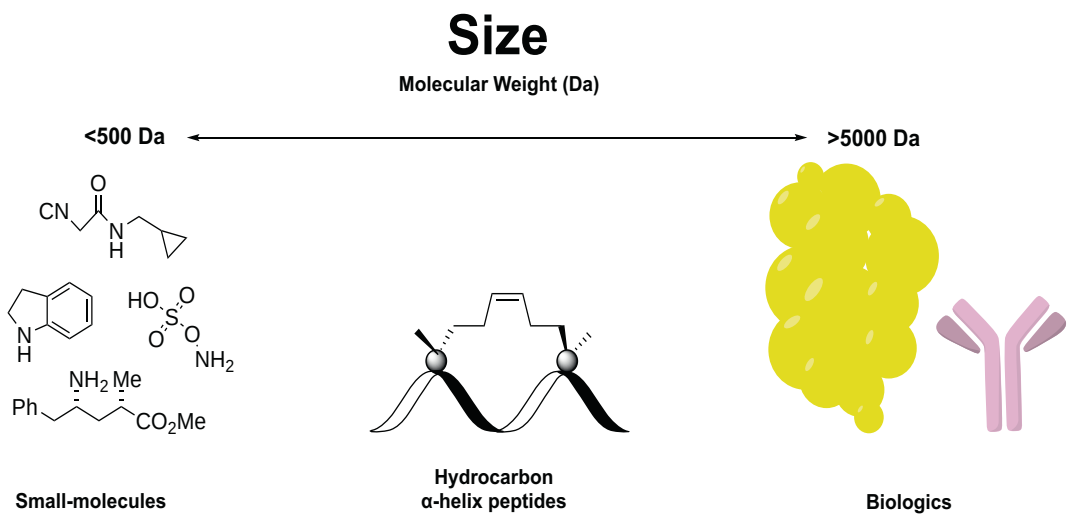

Fig. 1. The three classes of targeted medicines. The traditional small- molecules inhibitors were the first class discovered to inhibit different PPIs surfaces with MW of <500 Da and high bioavailability. Most of the biologics, the second class of PPI targeted molecules, have a MW of >5000 Da (eg. antibodies and growth hormones) aimed to overcome a broad range of diseases. Stapled α-helix peptides as a class address this gap in MW between small molecules and biologics, aiming to combine the oral bioavailability of small-molecules with the high specificity of biologics toward the target protein.

Structural knowledge of the target PPIs and mutagenesis data for residues at or near the binding interface are necessary to achieve a successful interruption of PPI partner proteins *in vivo*. Peptide design is based upon the ligand-target pair, in that the ligand retains its α-helical motif and is docked into shallow cleft surface of the target protein. Thus, stapled peptide inhibitors represent "dominant-negative" versions of the docking helix [5]. The peptide is then optimized by sequence modification "or stapling" to improve cell penetration and peptide efficacy to compete with the intracellular ligand protein, and it is crucial to position the cross-linking amino acids in such way that the targeted interface remains intact [5]. After evaluating the cellular uptake of the stapled peptides using live confocal microscopy, a broad spectrum of cellular and *in vivo* studies are applied to examine the therapeutic activity of the stapled peptides toward their targets. A flow-chart in Fig. 4 summarizes the development process of therapeutic peptides for biological study, from virtual design to *in vivo* mouse model analysis. Examples of stapled peptide created through the use of high-resolution structures are $SAHB_A$, based on BH3 domain of proapoptotic BID protein [25], SAH-p53, based on the p53-MDM2 interaction interface [29], SAH-gp41 double stapling peptide, targeting the HIV-1 virus and Enfuvirtide, the first decoy HR2 helix fusion inhibitor [30]. If the proteins involved in the PPIs of interest have no previous structures, Ala-scanning or residue conservation "in situ mutagenesis" can be used as a starting point to position the staple. If this information is also not available, then synthesizing and screening all stapling positions is advisable [5].

3. Chemical Synthesis of Stapled Peptides

As the synthesis of bioactive-stapled peptides started to widen, the approaches used also branched and allowed stapled peptides to be applied for various purposes such as target binding analyses, structure determination, proteomic discovery, signal transduction research, cellular analyses, imaging, and *in vivo* bioactivity studies [31]. Solid-phase peptide synthesis (SPPS) is a standard and commonly used chemical

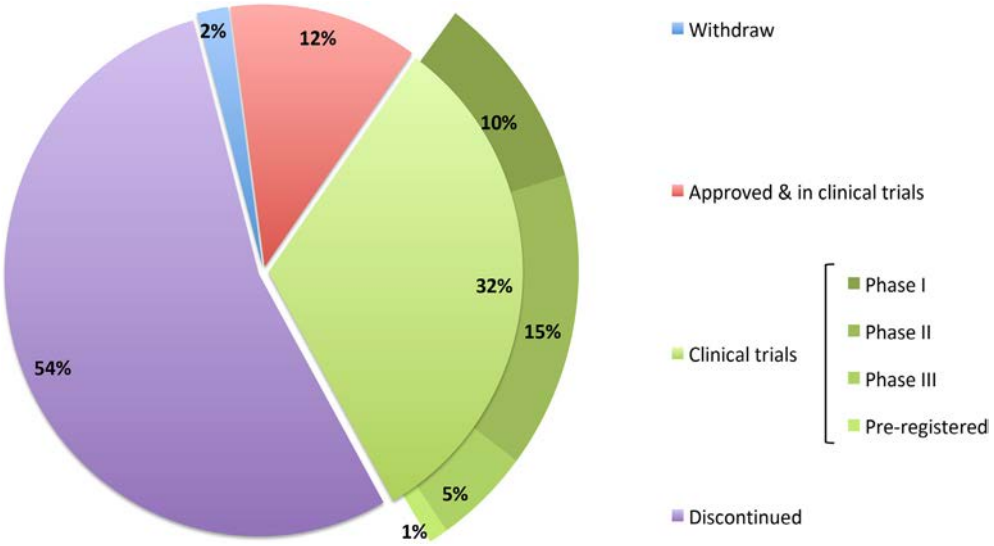

Fig. 2. Statistical representation of therapeutic peptides until March 2017. The numbers are indicated in percentage at each category with a total number of 484 medicinal peptides that were produced with development activity regulatory approval from major pharmaceutical markets as, the United States, Europe, and Japan. From these peptides 12% were approved, while 32% are in clinical trials and further classified as phases I, II, III and pre-registered. The highest percentage (54%; "Discontinued") category encompasses peptides terminated before approval. The lowest percentage 2% is the "Withdraw" category that refers to previously approved peptides that are no longer available in the market [18].

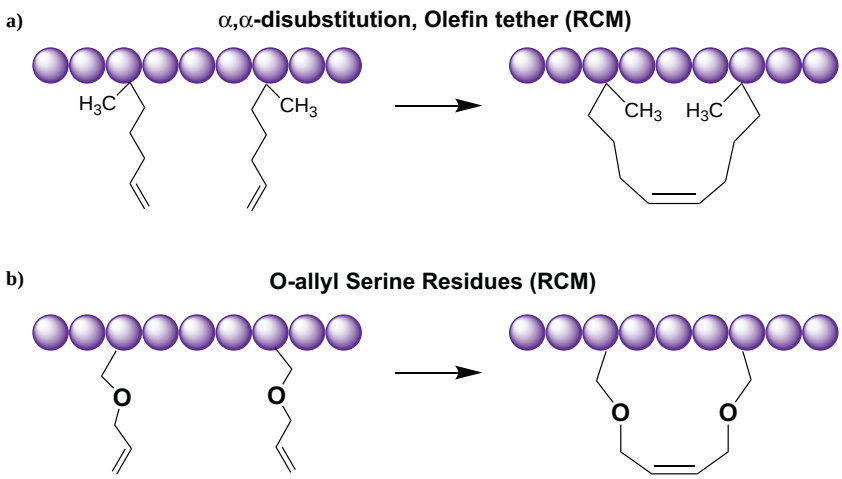

Fig. 3. Ruthenium-catalyzed ring-closing metathesis (RCM) reaction for peptides stapling was a) published for the first time by Verdine and Schafmeister in 2000 by engaging α,α-disubstituted non-natural amino acids harboring all-hydrocarbon tethers [19]. Their work was a continuation of b) Blackwell and Grubbs work in 1998 [24]; who performed ruthenium-catalyzed olefin metathesis for macrocyclisation of synthetic peptides using a pair of O-allylserine residues in a metathesis reaction.

procedure to synthesize α-helix peptides. The first required entity to start stapled peptides synthesis is a stock of non-natural amino acids building blocks with a variable length of the terminal olefin tethers. The choice of the non-natural amino acids will define the length, structure and the chemical functionalities of the stapled linker [14,32]. The helix backbone amino acids are protected with a base-labile fluorenylmethoxycarbonyl (Fmoc) to obtain *N*- α -Fmoc-protected amino acids, which are often offered with acid-labile side chain protecting groups that vary between the 20 amino acids. The side chain protecting groups of each amino acid for standard SPPS of stapled peptides are indicated in Table 1. After the synthesis of non-natural amino acids and peptide elongation during SPPS; ring-closing metathesis (RCM) of the stapled is performed.

SPPS has been automated using Fmoc chemistry to become an efficient and reliable method to yield hydrocarbon-stapled peptides of single or double stapling with different functionalities and experimental applications. However, SPPS has two main complications: First, efficiency is limited in longer peptides (>50 residues). These are more usually expressed using recombinant DNA technology, due to the unavailability of the N-terminal amine of the non-natural amino acids (mostly after naturally bulky residues like arginine or β- branched amino acids (valine, isoleucine, and threonine)). Additionally, extension of deprotection and coupling times with fresh reagent may be required in the synthesis of larger peptides. The second complication is that cross-reaction or progressive inaccessibility of the N-terminus due to on-resin aggregation could occur [31–33].

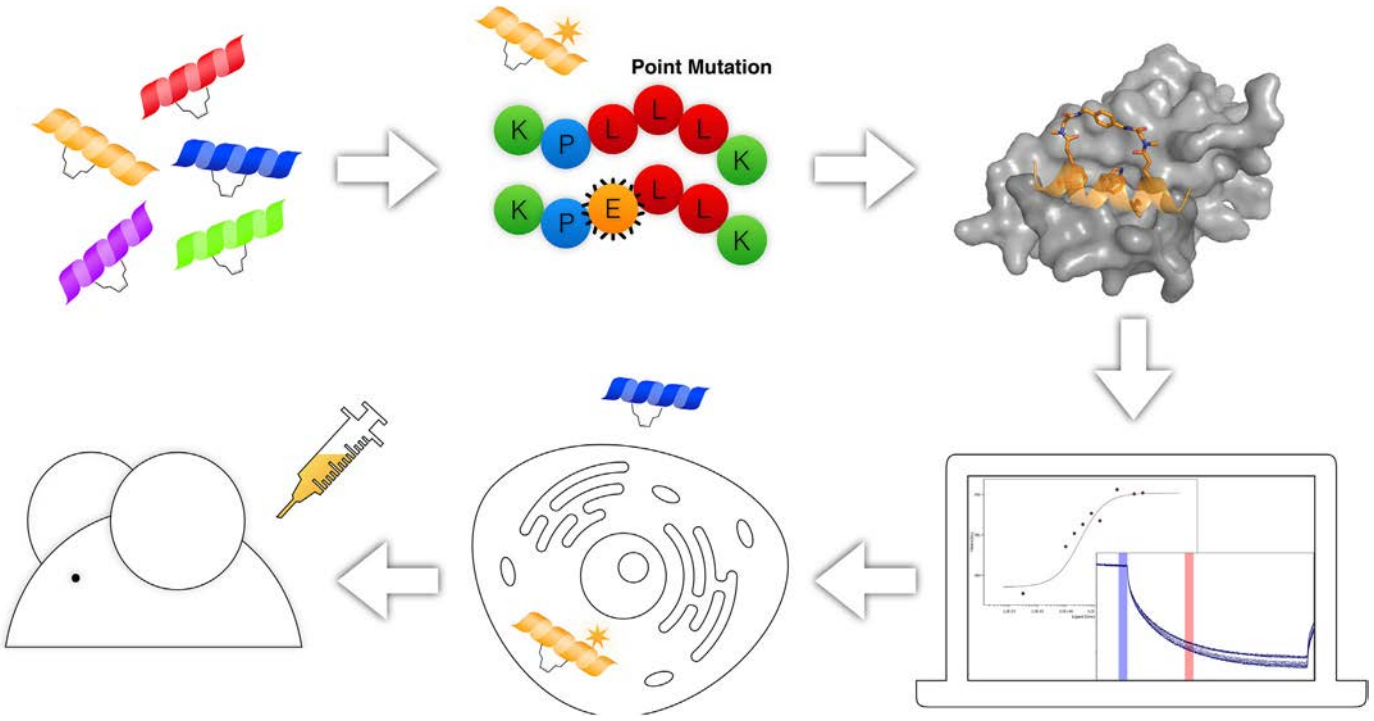

Fig. 4. Workflow of all hydrocarbon-stapled peptides generated for biological investigation. Computational designation of the peptides including *in-situ* mutagenesis to screen all possibilities based on previous reported structures, followed by *in vitro* biochemical, structural, and functional studies compromising peptides binding affinities measurements toward the target protein interface utilizing biophysical assays and crystallization trials. Potent binder peptides will be further tested for their cellular uptake and permeability using live confocal microscopy. Lastly, successful peptides are subjected to a broad spectrum of cellular and *in vivo* analyses, using mouse models of the studied disease.

Table 1
The acid-labile side chain protecting groups used in SPPS synthesis of stapled peptides.

Amino acid	Three letters-code	Side chain protecting group
Alanine	Ala	N/A
Cysteine	Cys	Trityl (Trt)
Aspartic acid	Asp	tert-Butyl (OtBu)
Glutamic acid	Glu	tert-Butyl (OtBu)
Phenylalanine	Phe	N/A
Glycine	Gly	N/A
Histidine	His	Trityl (Trt)
Isoleucine	Ile	N/A
Lysine	Lys	tert-Butoxy (Boc)
Leucine	Leu	N/A
Methionine	Met	N/A
Asparagine	Asn	Trityl (Trt)
Proline	Pro	N/A
Glutamine	Gln	Trityl (Trt)
Arginine	Arg	Pentamethyldihydrobenzofurane (Pbf)
Serine	Ser	tert-Butyl (OtBu)
Threonine	Thr	tert-Butyl (OtBu)
Valine	Val	N/A
Tryptophan	Trp	tert-Butoxy (Boc)
Tyrosine	Try	tert-Butyl (OtBu)

Initial screening of different types of stapling is required if structural-based knowledge is not available. As indicated previously in Section 2, prediction software can suggest the peptide α-helix template, then a group of constructs with differentially localized staples can be generated to determine the optimal staple placement. However, if the target PPIs interface is structurally well characterized, this structural data can be used for computational docking and designing of the desired template peptide to generate a panel of peptides with diverse stapling type and position. Stapling techniques could be divided into one-component or two-component stapling techniques, based on the side-chain linking reaction. During one-component stapling a direct bond will be formed between two non-natural amino acids side-chains, whereas two-component stapling involves a separate bifunctional linker to connect the side-chains of two non-natural amino acids [14]. The most commonly used technique for stapling is the one-component stapling technique - employing S-pentenylalanine at *i,i + 4* positions for one turn stapling or combining either R-octenylalanine/S-pentenylalanine or S-octenylalanine/R-pentenylalanine at *i,i + 7* positions. Other spacings for stapling were also accomplished upon chemical optimization, including *i,i + 3* and *i,i + 11* [14,31,32,34]. The common stapling positions are shown in Fig. 5.

There are several chemical procedures to enclose or stabilized the all-hydrocarbon linker into α-helix peptide such as, ring-closing metathesis, lactamisation, cycloadditions, reversible reactions and thioether formation. A brief summary for each methodology and some literature examples is provided below.

3.1. Ring-Closing Metathesis (RCM)

Blackwell and Grubb were the first to apply alkene ring-closing metathesis as a peptide stapling method. They described solution-phase metathesis, followed by hydrogenation of hydrophobic heptapeptides containing either *O*-allyl serine or homoserine residues with *i,i + 4* spacing (Fig. 6) [24]. Their study emphasized the feasibility of metathesis on helical peptide side-chain. Later in 2000, Schafmeister and his colleagues managed to conduct metathesis stapling using α,α-disubstituted amino acids carrying olefinic side-chains of different lengths and stereo-chemistry on solid phase prior to peptide cleavage from resin,

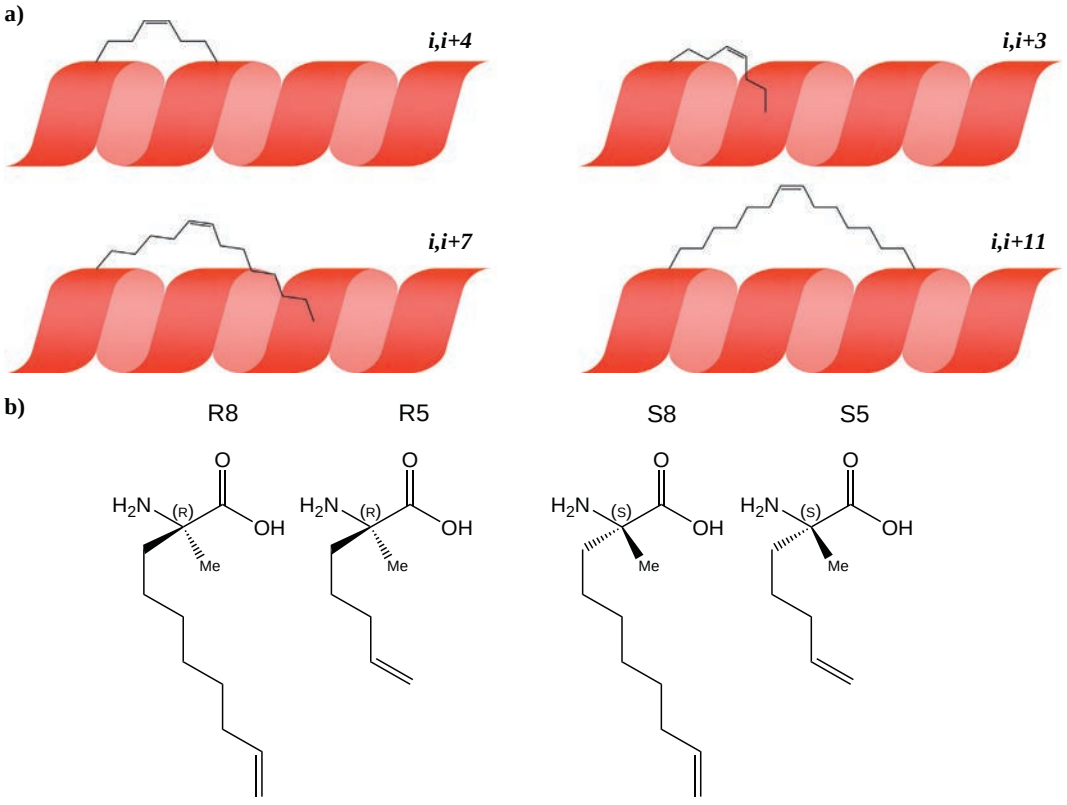

Fig. 5. a) The common stapling insertion positions for α-helix peptides. Combinations of two non-natural amino acids S5, R5, S8 and R8 are used for different positions of stapling the hydrocarbon linker. Employing S5/S5 at position *i,i + 4* is the most common stapling position on the same face of helix turn. For *i,i + 7* position, two combinations could be applied either S8/R5 or S5/R8. Synthetic chemistry evolved to introduced *i,i + 3* and *i,i + 11* as new possible positions for stapling in addition to double-stapling. b) The structures of the four designed amino acids used to introduce all-hydrocarbon staples into peptides. All possess an α-methyl group (Me) and an α-alkenyl group, but with opposite stereochemical configuration and different length at the alkenyl chain.

Fig. 6. RCM or ring closing metathesis reaction for synthesis of the all-hydrocarbon stapled peptide reported by Schafmeister et al. 2000, which increase peptides helicity as found by circular dichroism (CD) [19].

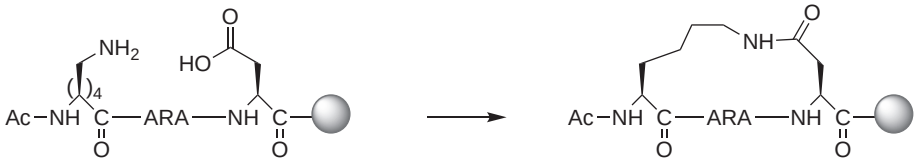

Fig. 7. A Lactamisation study that was conducted by Fairlie and co-workers on penta and hexa-peptides in order to optimize lactam stapling between Orn/Lys and Asp/Glu residues. It wasn't the first study for lactam optimization; however, the group was abled to systematically and quantitatively found the shortest peptide with retained helicity in water as judged by CD [39].

producing a large series of α, α-disubstituted non-natural amino acids S5, R5, S8 and R8 bearing olefin tethers that were used for different stapling positions of the hydrocarbon linker as shown in Fig. 5. The end products were a collection of *i,i + 4/7* peptides and they found that *i,i + 7* stapled peptides have higher helicity and stability over native and non-stapled peptides [19]. BID BH3 peptides that bind to BCL-2 family proteins are a successful product of metathesis stapling by Walensky et al. and they showed that the optimized stapled peptide has more stability than the native one, provoke apoptosis in leukemia cells, and inhibit the growth of human leukemia xenografts in mice [25]. p53-MDM2/MDMX dual inhibitor stapled peptides were reported by Sawyer and co-workers, who provided promising *in vitro* data for binding affinity, cellular activity and suppression of human xenograft tumors in animal models [35]. These findings are the basis of p53 optimized stapled peptides that have enter clinical trials.

Further, Verdine et.al introduced a unique form of multiple stapling, called stitches, in which two hydrocarbon staples immediately follow one another. This technique requires the use of the amino acid bispentenylglycine (B5) that forms a junction between the two staples and emerges from a common residue in the peptide. There are many possible combinations of stereochemistry and linker length in such a system. Various stitch combinations were studied rigorously and two systems, *i,i + 4 + 4* (S5 + B5 + R5) and *i,i + 4 + 7* (S5 + B5 + S8), appeared the most effective for helix stabilization. A peptide with the latter stitch construction was found to have superior helicity and cell penetration compared with an *i,i + 7* stapled analogue [36].

Optimization and extensive development in hydrocarbon stapling approach allow stapling at *i,i + 3/4/7* spacings. Regardless of the many examples in literature of successful hydrocarbon stapling, there is no guarantee that stapling will enhance peptide stability, cell penetration and binding to the target. Extensive optimization is needed in order to discover a staple peptide with the desired features.

3.2. Lactamisation

Stabilization of an α-helix can also be accomplished through side-chain intramolecular amide-bond formation between *i,i + 4* spaced amine- and carboxy-side chain amino acids. Lactamisation was first studied by Felix et al. in 1988 [37], in which they coupled Lys and Asp residues side-chains in a growth hormone releasing factor short congener. Growth hormone helicity and activity were conserved post macrocyclisation, which were measured by NMR and circular dichroism (CD) (both methods that can be used for analyzing the secondary structure of peptides and proteins in aqueous solution) [38]. Since then, numerous studies applied lactamisation and amide linkage on different chain length and positions, with the intention of generating a stable helix for different systems. For example, a lactam stapling optimization study on penta/hexapeptides between Orn/Lys and Asp/Glu residues, carried out by Fairlie and co-workers (Fig. 7) [39], examined the shortest possible peptide with α-helix reinforced structure in water. Subsequently, the Fairlie group applied their finding on different targets, including inhibition of respiratory syncytial virus with double lactam-stapled peptide in 2010 with improved antibacterial activity. Another target was the nociceptin hormone studied in the same year, in which lactam-stapled peptide induced higher ERK phosphorylation in mouse cells and thermal analgesia [22]. Norton and co-workers also examined several Asp/Lys lactam-stapling combinations at *i,i + 4* position on μ-conotoxin KIIIA, a natural peptide from mice that acts as a potent analgesic by binding voltage-gated sodium channels (VGSCs), where they found that stapled peptides have different level of helicity and inhibitory activity on variable VGSC when examined in *Xenopus laevis* oocytes [40]. From a chemical perspective, lactam stapling is easier to obtain and incorporate due to proteogenic amino acids when compared to other stapling techniques, which require non-proteogenic amino acids. A drawback is that an extra orthogonal protecting group is needed for selective deprotection of the amino

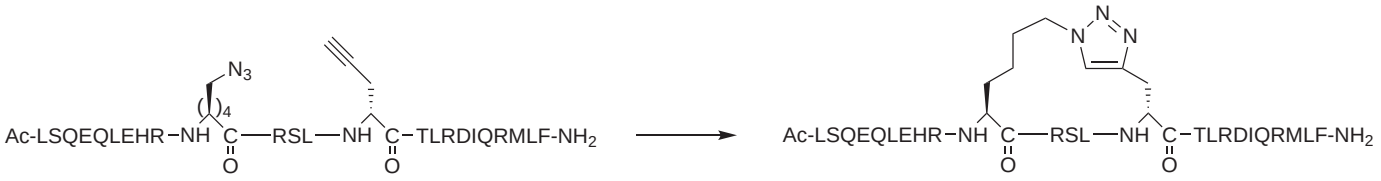

Fig. 8. Optimized CuAAC-stapled peptide was successfully developed to inhibit the BCL9 oncogenic interaction. After screening different stapling length, Wang and co-workers concluded that five units of methylene was optimal stapled peptide for BLC9 inhibition [43].

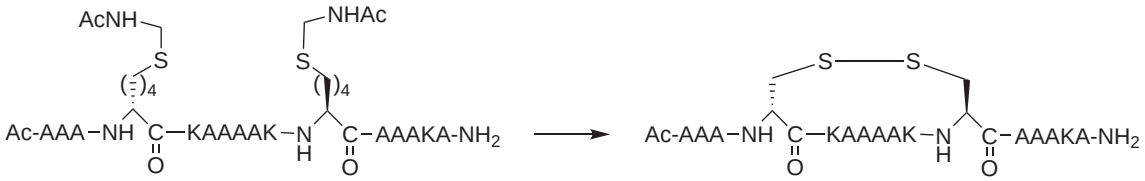

Fig. 9. Schultz and co-workers described an *i,i + 7* stapling methodology using disulphide bridges between D and L amino acids bearing thiol-side chains. The amino acids were connected with acetamidomethyl (Acm) protecting groups, deprotected and then oxidised with iodine to give a disulphide stapled peptide. CD spectra of disulphide stapled peptides exhibited a high level of α-helicity in comparison to the Acm-protected precursors that were significantly less helical [45].

acid functionalities prior to lactamisation. Another limitation of this technique should be mentioned, which is the lactamisation stapling of Lys and Asp residues. Stapling at these residues is only compatible with *i,i + 4* spacing with longer linkages that required modified amino acids with longer side-chains. From a biological point of view, and based on a large number of studies on peptide lactamisation, this stapling technique can create therapeutic peptides with superior bioactivity. However, most of their targets are either extracellular or membrane-bound, suggesting that lactamisation stapling has no potential to improve cell penetration [14].

3.3. Cycloadditions

Cu (I)-catalyzed azide–alkyne cycloaddition (CuAAC) or the "Click" reaction is another mechanism of peptide stapling, it is also known as biocompatible ligation technique [41]. The first research group who applied CuAAC to generate α-helix structures between *i,i + 4* spacing within peptides were Chorev, D'Ursi and co-workers in 2010, based on parathyroid hormone-related peptide [42]. Subsequently, many groups used this type of stapling in order to determine the best linker length, including Wang and co-workers, who found that five methylene units were the optimum staple length to inhibit the oncogenic BCL9-beta-catenin PPI (Fig. 8). A further significant result, reported by the same team, of the Click reaction was based on triazol-position screening along a peptide targeting the same oncogenic protein, beta-catenin, to generate a library of stapled peptides exhibiting different *in vitro* binding affinities and helicity [43]. Madden et al., used an unusual cycloaddition via UV-induction between tetrazoles and alkenes to hinder p53-MDM2/MDMX interaction. The stapling reaction took place between *i,i + 4* by exposing unprotected linear peptides to UV irradiation in solution, which resulted in stapled peptides displaying higher affinity toward MDM2/MDMX in a fluorescence polarization assay (FP). However, these peptides were not cell permeable. This problem could be overcome by modifying a number of the peptide amino acids to Arg, whereby cellular uptake and moderate p53 activity were achieved [44]. Generally, stapling with cycloaddition chemistry shows a promising future, in that triazol- stapled amino acids are accessible and CuAAC is well established. In the example of UV-induced reactions, the method is simple to apply but requires extra analysis that might affect applicability in other biological systems.

3.4. Reversible Reactions

Using disulphide bridges between two Cys residues as stapling technique was first introduced by Schultz et al. at *i,i + 7* positions. The disulfide bridge was formed between D and L-amino acids having thiol-side chain, followed by the addition of acetamidomethyl (Acm) protecting groups, protection and oxidization with iodine (Fig. 9). The helicity of disulfide-stapled peptides was higher when compared with the Acm-protected precursors, as displayed in CD spectroscopy [45]. Although disulfide stapling was the earliest reported stapling technique, little was concluded due to the instability of the disulphide stapled peptides in reducing environments, which restrict their application in intracellular targets. However, stapling with oxime linkages [46] and two-component bis-lactam and bis-aryl stapling techniques [47,48] were found to be superior to the analogous disulphide stapling. Recently, Wang and Chou demonstrated the possibility of stapling and macrocyclization using thiol-en between two Cys residues an α, ω-diene in high yields (an unsaturated hydrocarbon containing two double bonds between carbon atoms), which allowed stapling of both expressed/unprotected and synthetic peptides. This group applied their discovery to the p53-MDM2 PPI and successfully synthesized stapled peptides with both *i,i + 4* and *i,i + 7* linkages, applying this method in the stapling of large peptides and proteins. Development in reversible stapling is slow, but efforts in applying this method in biological dynamic covalent chemistry are under active investigation.

3.5. Thioether Formation

The reaction between Cys thiol and alpha-bromo amide groups has been developed as a protocol for peptide stapling by Brunel and Dawson [49]. This linkage was designed to mimic the ring size of previously reported lactam staples, but a thioether link was hosted into gp41-peptide epitopes as an approach to establish an HIV vaccine. Successful staples were created in both *i,i + 3* and *i,i + 4* linkages and a peptide with *i,i + 3* stapling (Fig. 10) demonstrated a higher helicity over unstapled and lactam-stapled peptides *i,i + 4*. Moreover, after optimization the stapled peptide bound to a gp41-specific antibody (4E10) more effectively than the uncyclised peptide [50]. These findings illustrate the efficiency of thioether stapling with shorter distance *i.e. i,i + 3*, while suggesting that lactam staples are more suitable for *i,i + 4* stapling.

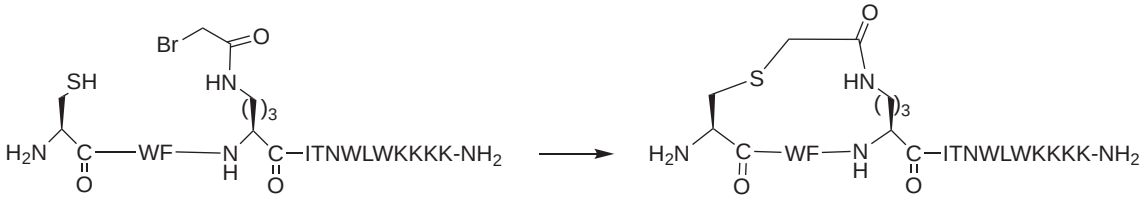

Fig. 10. Thioether stapling method was reported by Brunel and Dawson in 2005. They demonstrated the reaction of Cys thiol and alpha-bromo amide groups to report a *i,i + 3* thioether stapled peptide that inhibited HIV fusion using the gp41 epitopes as template for peptide synthesis [49].

4. Structural Insight of Stapled Peptides Target Protein-Protein Interaction (PPI) in the PDB

The number of peptides entering clinical trials has increased over the last 35 years, with an average peaking in 2011, when over 22 peptides/year were successful in entering clinical development [18]. This evolved from technology maturation and advances in synthetic chemistry and purification of peptides, in parallel with improvements in biophysical and molecular pharmacological methods. However, there is a limited number of high-resolution structures of staple peptides in complex with their targets in the protein database (RCSB www.rcsb.org), as of July 2018 [51]. There are 67 "stapled peptides" structures, of which 58 are based on X-ray diffraction (83%) and 9 on NMR studies (17%). When limiting the analysis to *Homo sapiens*, our search found 43 structures, targeting a limited range of PPIs, of which the majority are of the p53-MDM2/MDMX interaction, the BCL-2 family (including the MCL-1 BH3 domain), estrogen receptor and human immunodeficiency virus type 1 (HIV-1). Other druggable interfaces of interest were kinases [52,53], insulin [54], tankyrase-2 [55], growth factor receptor-bound protein 7 (Grb7) [56], the Fc portion of human IgG [57], eIF4E protein [58] and transducin-like enhancer (TLE) proteins [59]. MDM2 and its homolog MDMX represent 18.6% of total X-ray structures in protein data bank, which indicates their importance as the main negative regulators of p53 ("The Guardian of the genome") since it behaves as a hub protein [60]. This escalation in stapled peptide drug discovery has crossed over into the traditional focus upon endogenous human peptides to include a broader range of structures identified through medicinal chemistry efforts. Not surprising, today over 150 stapled peptides are in the active development of human clinical studies [18].

The analysis presented in Table 2 provides a list of the crystal structures belong to therapeutic stapled peptides, which mimic the native peptides in complex with their target protein interfaces. The table also gives an overview of the PDB structure code, name of stapled peptide and biophysical assays that are used to measure the binding dissociation constant (K_d) of the stapled peptide to the target protein.

Not all staples interact with the target protein surface via commonly known chemical interactions; instead they can induce conformational changes to either the synthetic α-helix peptide or the target protein interface, specifically the amino acids residues involved in PPIs. These changes stabilize and fix the helical peptide in a potent binding mode within the target interface. A limited number of stapled peptides have different interactions with their intracellular targets, which contributes to their high specificity, stability and makes these peptides promising target therapies for human diseases. Table 3 underlines the role of the stapled linker in binding to the target protein surface and indicates if it is involved in any interaction with the target surface residues via Van der Waals, hydrogen/disulfide bonds or π-π interactions. All of these interactions were inspected from the crystal structures of the stapled peptides in complex with the target protein surfaces. Examples of these peptides will be discussed extensively in the next sections to highlight the evolution of medicinal chemistry techniques.

4.1. SAH-p53-8: Stapled p53 Peptide Binds Potently to Human MDM2

p53, the main tumor suppressor, which is mainly negatively regulated by the E3 ubiquitin ligase MDM2. Although p53 is mutated or inactivated in >50% of human cancers, the other 50% retain WT-p53. Therefore, the p53: MDM2 PPIs is a promising and confirmed target for drug discovery and cancer therapy. This can be accomplished by discovering a potent MDM2 binder in order to prevent its binding to p53 and thereby restore its biological function. In 2012, Baek and coworkers were able to resolve a high-resolution structure of a stapled peptide inhibitor in complex with MDM2 (SAH-p53-8 (PDB 3V3B)) [62]. This peptide was synthesized following ring-closing olefin metathesis (RCM) at $i,i+7$ stapling positions between residues Asn20 and Leu26. As anticipated by molecular dynamics (MD), the crystal structure revealed an extended region of the helical peptide from residues 19–27 in the bound state that was not seen in other peptides with lower affinities toward MDM2. Moreover, the bound peptide induced minor changes in MDM2, specifically at the side chain of Met62 (which folds away from the p53 binding pocket, to make space for the staple), Val93 (which shifts inside the binding pocket) and the side chain of Tyr100 that is found in a "closed" form. However, the α-helix peptide is located in the same position as the native helix of p53, orienting the three residues critical for binding (Phe19, Trp23 and Leu26) in the correct location (Fig. 11). Remarkably, the aliphatic staple intimately interacts with the protein and is located directly over the Met50-Lys64 helix and contributes *ca.* 10% of the peptide-Mdm2 total surface contact area. Additionally, the staple shields a H-bond between Trp23 and Leu54 from solvent competition (Fig. 12). Two novel features were discovered in the complex structure, first an extended hydrophobic interface of the staple linker with Leu54, Phe55, Gly58, and Met62 of Mdm2. The second feature is that the staple displaced a common water molecule present in most MDM2 structures, which forms H-bonds with Gln59-N and Phe55-O. The later displacement likely entropically stabilizes the complex during binding and contributes to SAH-p53-8 tight binding as evidenced by an FP assay showing a K_d of 55 nM. Lastly, stapling increases peptide helicity during binding in relation to that of native p53 - influencing residue Leu26, which plays an important role in MDM2 binding. Additionally, the researchers concluded that the long stapling $i,i+7$ enhanced helical conformation and affinity as suggested by previous studies [19]. Subsequent to the discovery of SAH-p53-8, several stapled peptides, such as sMTide-02 [99] and ASTP-7041 [35], showed potent binding toward MDM2 with K_d values of 34.35 and 0.91 nM, respectively. Additionally, both peptides (in addition to VIP-84 (another stapled peptide targeting MDM2: p53)) showed cellular permeability when tested using a nanoBRET (Bioluminescence Resonance Excitation Transfer) live cell assay. Screening various lipid based formulations, the cellular uptake of VIP-84 was shown to be enhanced, as well as its biological activity, which was linked to vesicular or endosomal escape of the stapled peptide through the cell membrane [100].

4.2. MDM2 Double Macrocyclization Stapled Peptide: Fast Selection of Cell-Active Inhibitor

Following on from the SAH-p53-8 potent peptide inhibitor, Lau et al. managed to synthesize a stapled peptide-E1 by applying a novel stapling technique [64]. This technique is based on double Cu-catalyzed azide–alkyne cycloaddition (CuAAC) and followed two-component strategies, in that the staple and α-helix peptide are separated before cyclisation. This was combined with click chemistry to generate a peptide with variable functional staples. The team used the p53-MDM2 interaction as a model, since that target has been well investigated as an oncogenic therapy for cancers with overexpressed MDM2. For optimum inhibitor screening, and to ensure fast and easy selection for the best peptide, cyclisation was conducted *in situ* and directly in primary cells medium using a 96-well assay. This approach eliminated the extra purification step required in other two-component strategies and provided a first example of stapling within a biological environment. The first stapled peptide A1 was synthesized by linking diyne 1 to p53-derived diazidopeptide A to produce A1 with 60% yield. Different peptide variants B-E were tested *in situ* to define a peptide with the highest p53 activation, showing that the E+1 stapled peptide was the most potent activator within cells. The binding affinity of the E1 peptide was measured using two biophysical assays (FP and ITC) determining K_d values of 7.5 ± 0.7 and 12 ± 3 nM, respectively. The crystal structure of E1-MDM2 (17–108, E69A/K70A) complex at 1.9 Å resolution elucidated the helical structure of E1 orienting the three hydrophobic key residues (Phe19, Trp23 and Leu26) in the correct positioning for MDM2 binding (PDB 5AFG), in a manner broadly similar to that of the p53 native peptide (Fig. 13a). The bis (triazolyl) staple was discovered in an *anti*

Table 2
List of structural-resolved stapled peptides in complex with PPI targets from RCSB-PDB.

Target	PDB ID	Binding Assay	Peptide	K_d (nM)	Ref.	
					X-ray	NMR
Human MDM2/4	1YCR	ITC	p53-WT Residues (15–29)	600	[61]	NA
	3V3B	FP	SAH-p53-8 Stapled peptide	55	[62]	NA
		ITC		12		
	4UMN	FP	M06 Stapled peptide	63 ± 17.8	[63]	NA
	5AFG	FP	E1 Stapled peptide	7.5 ± 0.7	[64]	NA
	4UE1	FP	YS-1 Stapled peptide	9.9 ± 1.5	[65]	NA
	4UD7	FP	YS-2 Stapled peptide	7.4 ± 1.5	[65]	NA
	5XXK	FP	M011 Stapled peptide	6.3 ± 2.9	[66]	NA
	5VK0	–	PMI	–	[67]	NA
	5VK1	–	PMI	–	[67]	NA
MCL-1/BCL-2	3MK8	FP	MCL-1 $SAHB_D$ Stapled peptide	10 ± 3	[68]	NA
	5C3F	FP	BID-MM Stapled peptide	153 ± 12	[69]	NA
		SPR		107 ± 29		
	5C3G	SPR	BIM-MM Stapled peptide	460 ± 232	[69]	NA
	5W89	FP	SAH-MS1-18 Stapled peptide	25 ± 7	[70]	NA
	5W8F	FP	SAH-MS1-14 Stapled peptide	80 ± 5	[70]	NA
	5WHI	–	BCL-1 Apo	–	[71]	NA
	5WHH	Streptavidin pull-down	D-NA-NOXA SAHB Stapled peptide	–	[71]	NA
Estrogen Receptor	2YJD	SPR	SP1	ERβ/1.99 μM αER/674	[72]	NA
	2YJA	SPR	SP2	ERβ/632 αER/352	[72]	NA
	5DXB	SPR	SRC2-SP1	530	[73]	NA
	5HYR	SPR	SRC2-SP2	42	[73]	NA
	5DX3	SPR	SRC2-SP3	39	[73]	NA
	5DXE	SPR	SRC2-SP4	–	[73]	NA
	5DXG	SPR	SRC2-SP5	–	[73]	NA
	2LDA	–	SP2	–	NA	[72]
	2LDC	–	SP1	–	NA	[72]
	2LDD	–	SP6	ERβ/155 αER/75	NA	[72]
	5WGD	–	SRC2-LP1	–	[74]	NA
	5WGQ	–	SRC2-BCP1	–	[74]	NA
Aurora-A	5LXM	ITC	Stapled TPX2 peptide 10	0.18 μM	[73]	NA
Tankyrase-2	5BXO	FP	Cp4n2m3	0.6 ± 0.01 μM	[55]	NA
	5BXU	FP	Cp4n4m5	2.8 ± 0.1 μM	[55]	NA
Grb7	5D0J	SPR	G7-B4NS peptide	4.93 ± 0.03 μM	[56]	NA
	5EEL	SPR	G7-B4 peptide	0.83 ± 0.006 μM	[56]	NA
	5EEQ	SPR	G7-B1 peptide	1.5 ± 0.01 μM	[56]	NA
Replication proteinA	4NB3	FP	Peptide-33	0.022 ± 0.005 μM	[75]	NA
eIF4E	4BEA	SPR	sTIP-04 Stapled peptide	5 ± 0.7	[58]	NA
		FP		11.5 ± 3.6		
β-catenin	4DJS	FP	aStAx-35	13 ± 2.0	[76]	NA
hDcn-1	3TDZ	ITC	$hCul1^{WHB}$: $hDcn1^{P}$: Acetyl-$hUbc12^{1-12}$(5:9 Staple)	0.15 μM	[77]	NA
Insulin	3KQ6	Receptor Binding Assays	[$HisA^4$, $HisA^8$] insulin	IGF-1R/0.05 ± 0.01 IR/125 ± 18	[54]	NA
ks-vFLIP	5LDE	ITC	spIKKγ-Stapled peptide	30.4 ± 3.8 μM	[52]	NA
TLE1	5MWJ	ITC	Peptide18	522 ± 39.6	[59]	NA
human IgG1 Fc	5U66	SPR	LH1	~1 ± 0.5 mM	[57]	NA
Ca_V β subunit	5V2P	ITC	AID-CAP Stapled peptide	5.1 ± 1.6	[78]	NA
	5V2Q	ITC	AID-CEN Stapled peptide	5.2 ± 1.5	[78]	NA
NCOA1	5Y7W	–	YL-2	–	[79]	NA
Saccharomyces cerevisiae	5NXQ	FP	Sld5 CIP A2	0.32 ± 0.02 μM	[80]	NA
	4HU6	–	GCN4-p1(7b)	–	[81]	NA
CRPs (Plants)	5NGN	–	Lyba2	–	[82]	NA
HIV-1	4NGH	–	SAH- MPER(671-683KKK)(q)pSer	–	[13]	NA
	4NHC	–	SAH-MPER(671-683KKK)(q)	–	[13]	NA
	4U6G	–	SAH-MPER(662-683KKK)(B,q)		[13]	NA
	8HVP	–	Ua-I-OH 85548e	–	[83]	NA
	7HVP	–	JG-365	–	[84]	NA
	2L6E	Total buried surface	NYAD-13	1 μM	NA	[85]
	2JUK	–	GNB	–	NA	[86]
	1ZJ2	–	HIV-1 frameshift site RNA	–	NA	[87]
	1PJY	–	HIV-1 frameshift inducing stem–loop RNA	–	NA	[88]
Brevibacillus Bacteria	4OZK	–	LS	–	[89]	NA
Zebrafish MDM2/X	4N5T	Biacore	ATSP-7041	MDM2/0.91 MDMX/2.31	[35]	NA
Plasmodium falciparum	4MZJ	–	pGly[801–805]	–	[90]	NA
	4MZK	–	pGly[807-811]	–	[90]	NA
	4MZL	–	HSB myoA	–	[90]	NA
XRMV	4JGS	–	γ-XMRV TM retroviral fusion protein	–	[91]	NA
MPMV	4JF3	–	β-MPMV TM retroviral fusion protein	–	[91]	NA
Salmonella	1Q5Z	–	SipA	–	[92]	NA

(continued on next page)

Table 2 (*continued*)

Target	PDB ID	Binding Assay	Peptide	K_d (nM)	Ref.	
					X-ray	NMR
Synthetic collagen	3P46	–	SS1	–	[93]	NA
EphA2-Sam/Ship2-Sam complex	6F7M	MST	S13ST	Ship2-Sam/52.2 ± 0.7 μM	NA	[94]
	6F7N	MST	S13ST (short)	Ship2-Sam/No binding	NA	[94]
	6F7O	MST	A5ST	Ship2-Sam/No binding	NA	[94]
Human Cul3-BTB	2MYL	FP	$Cul3^{49\text{-}68EN}$	620 ± 177	NA	[95]
	2MYM	FP	$Cul3^{49\text{-}68LA}$	305 ± 100	NA	[95]
SIV	2JTP	–	RNA stem-loop	–	NA	[96]
α-helical hairpin proteins	1EI0	–	P8MTCP1	–	NA	[97]
De novo proteins	2M7C	–	Cp-T^2C3b	–	NA	[98]
	2M7D	–	(P12W)-T^2C16b	–	NA	[98]

regioisomer and four hydrophobic interactions were found with the protein surface residues: Leu54, Phe55, Gln59 and Met62. This mode of binding was similar to previously reported structure PDB: 3V3B (described in Section 4.1) indicating that both staples are sited at the rim area of the p53-binding pocket, where Phe55 is the most important residue (Fig. 13b). The proteolytic stability, cellular uptake and toxicity of E1 peptide were evaluated, in which it showed high stability in a chymotrypsin assay, significant cellular permeability observed by confocal microscopy and did not show non-specific toxicity as determined in an LDH leakage assay.

4.3. Specific MCL-1 Stapled Peptide Inhibitor as Apoptosis Sensitizer in Cancer Cells

The members of BCL-2 family known to have an anti-apoptotic role in cells are considered to be key pathogenic proteins in human diseases categorized by uncontrolled cell survival - such as cancer and autoimmune disorders. The MCL-1 protein belongs to this family and supports cell survival by trapping the apoptosis- inducing BCL-2 homology domain 3 (BH3) α-helix of pro-apoptotic BCL-2 family members. Cancer cells utilize this physiological phenomenon by overexpressing anti-apoptotic proteins to guarantee their immortality. As a result, developing an inhibitor to block the hydrophobic pocket of the anti-apoptotic proteins from binding the BH3 α-helix could lead to the discovery of a successful drug. By mimicking BH3 α-helix, several small molecules compounds were synthesized to inhibit anti-apoptotic proteins and some are undergoing clinical trials (including ABT-263, obatoclax, and AT-101). Most target three or more anti-apoptotic member proteins, except the ABT-199 small molecule inhibitor, which has a high potency and specificity to the BCL-2 protein with a $K_i < 0.010$ nM. ABT-199 was discovered through reverse engineering of navitoclax and keeping similar hydrophobic interactions but modifying the electrostatic interaction with Arg103 (specific to BCL-2 not BCL-XL) [101]. Furthermore, ABT-199 has antitumor activity against different cancers as non-Hodgkin's lymphoma (NHL) [101], refractory chronic lymphocytic leukemia (CLL) [102,103], and BCL-2–dependent acute lymphoblastic leukemia (ALL) [101] *in vitro*. The same positive results were found *in vivo* when ABT-199 was tested on a wide spectrum of xenograft mouse models harboring human hematological tumor (RS4;11), B cell lymphoma with the t(14,18) translocation [101] and mantel cell lymphoma (MCL) [101,104].

Nonetheless, the topography of the binding groove and the amino acids residues involved in the protein interaction of BH3 helix determine the specificity of the anti-apoptotic protein-binding partner. Therefore, the need to discover an inhibitor that selectively targets the interacting surface, which is large and complex, is essential. Walensky and his group [68] selected MCL-1 as their research target, due to its survival role in a wide-range of cancers and protein overexpression that has been linked to the pathogenesis of diverse refractory cancers (including multiple myeloma, acute myeloid leukemia, melanoma and poor prognosis breast cancer [105–108]). This group was able to synthesize a highly potent stapled peptide (MCL-1 $SAHB_D$), which selectively binds MCL-1 and prevent it from suppressing the apoptosis pathway and sensitizing caspase-dependent apoptosis within cancer cells. A library of stapled alpha-helices of BCL-2 domain peptides was synthesized based on the BH3 domain of human BCL-2 family and stapling was located at the $i,i + 4$ positions using ring-closing metathesis (RCM). To define the binding and specificity of BH3 helix and MCL-1 alone, alanine scanning, site-direct mutagenesis and staple scanning were performed; the results indicated that MCL-1 $SAHB_D$ has the highest helicity ~90% and strongest binding, with a K_d of 10 nM as determined by an FP assay. The complex structure of the stapled peptide with MCL-1ΔNΔC was solved at 2.3 Å resolution (PDB 3MK8) and showed that MCL-1 $SAHB_D$ is present in a helical conformation and interacts with the MCL-1 canonical BH3-binding pocket. The peptide α-helix conserved residues L213, V216, G217, and V220 make a direct hydrophobic contact with the MCL-1 interface that is consistent with many BH3 domains. These hydrophobic interactions are reinforced by a salt bridge between MCL-1 $SAHB_D$ Asp218 and MCL-1ΔNΔC Arg263 (Fig. 14). Interestingly, the hydrocarbon staple with alkene *cis* conformation made a distinct hydrophobic contact with the edge of the MCL-1 binding site. Moreover, the methyl group explores a groove comprising Gly262, Phe318, and Phe319 of MCL-1 and additional contact was found between the staple aliphatic side chain and the edge of the main interaction site (Fig. 15). All of these structural evidence indicate the role of the staple in the high affinity binding of the peptide and its ability to provide biological specificity toward MCL-1. This group also demonstrated the capacity of MCL-1 $SAHB_D$ to effectively sensitize mitochondrial apoptosis *in vitro* using wild type and *Bak*−/− mitochondria mouse models and in OPM2 cells by measuring the dissociation of native inhibitory MCL-1/BAK complexes using FP assay. In comparison to ABT-199, the MCL-1 $SAHB_D$ stapled peptide shows good cell permeability and has the capacity to sensitize cancer cells to apoptosis when tested on Jurkat T-cell leukemia and OPM2 cells, underscoring the clinical relevance of these findings. However, the MCL-1 stapled peptide has not yet been evaluated in clinical trials.

4.4. Stapled Peptides SP1, SP2 Inhibit Estrogen Receptor ERβ

Estrogen receptor (ER) is a steroid hormone receptor that belongs to the nuclear receptor (NR) superfamily class. In addition to the receptor's role in reproduction regulation, ER has a regulatory role in other pathways in different systems such as the central nervous system, maintenance of bone density and immunity. Thus, ER is an attractive target for diseases primarily in breast cancer, endometrial cancer and osteoporosis [109–111]. Structurally the receptor existed in two isoforms (ERα and ERβ), in which both have a similar domain organization - namely an N-terminal transactivation (AF1) domain, a well-conserved DNA binding domain, and a C-terminal ligand-binding domain (LBD). Dependent upon the bounded ligand, the ER receptor has two different states that induce changes in the structure, stability and interaction of the LED with a co-activator protein. When ER is in an agonist-bound

Table 3
The binding role of the staples in X-ray structures from RCSB-PDB.

Target	PDB ID	Peptide	Cyclisation Method	K_d (nM)	Staple Interaction	Ref.
Human MDM2	1YCR	p53-WT Residues (15–29)	–	600	–	[61]
	3V3B	SAH-p53-8 Stapled peptide	RCM/*i,i* + 7 position	55	Hydrophobic contacts with Leu54, Phe55, Gly58, and Met62 of MDM2	[62]
	4UMN	M06 Stapled peptide	RCM/*i,i* + 7 position	63 ± 17.8	Hydrophobic contacts with Leu54, Phe55 and more closely with Gly 58 of MDM2	[63]
	5AFG	E1 Stapled peptide	CuAAC cycloaddition "Click-reaction"	7.5 ± 0.7	Hydrophobic contacts with Leu54, Phe55, Gln59 and Met62 of MDM2	[64]
	4UE1	YS-1 Stapled peptide	RCM/*i,i* + 4 position	9.9 ± 1.5	None	[65]
	4UD7	YS-2 Stapled peptide	RCM/*i,i* + 4 position	7.4 ± 1.5	None	[65]
	5XXK	M011 Stapled peptide	RCM/*i,i* + 7 position	6.3 ± 2.9	Hydrophobic contacts with Leu54, Phe55 and more closely with Gly 58 of MDM2	[66]
Zebrafish MDM2/X	4N5T	ATSP-7041	RCM/*i,i* + 7 position	Mdm2/0.91 MdmX/2.31	Van der Waals contacts with Lys47, Met50, His51, Gly54, Gln55, and Met58 of MDMX	[35]
MCL-1/BCL-2	3MK8	MCL-1 $SAHB_D$ Stapled peptide	RCM/*i,i* + 4 position	10 ± 3	Hydrophobic contacts with G262, F318, and F319 of MCL-1	[68]
	5C3F	BID-MM Stapled peptide	RCM/*i,i* + 4 position	153 ± 12 107 ± 29	None	[69]
	5C3G	BIM-MM Stapled peptide	RCM/*i,i* + 4 position	460 ± 232	None	[69]
	5W89	SAH-MS1-18 Stapled peptide	RCM/*i,i* + 4 position	25 ± 7	None	[70]
	5W8F	SAH-MS1-14 Stapled peptide	RCM/*i,i* + 4 position	80 ± 5	None	[70]
	5WHH	D-NA-NOXA SAHB Stapled peptide	RCM/*i,i* + 7 position	–	None	[71]
Estrogen Receptor	2YJD	SP1	RCM/*i,i* + 4 position	1.99 μM	Van der Waals contacts with Val307, Ile310, and Leu490 of ER_{β}_LBD	[72]
	2YJA	SP2	RCM/*i,i* + 3 position	352	Van der Waals contacts with Val307, Ile310, and Leu490 of ER_{β}_LBD	[72]
	5DXB	SRC2-SP1	RCM/*i,i* + 4 position	530	None	[73]
	5HYR	SRC2-SP2	RCM/*i,i* + 4 position	42	None	[73]
	5DX3	SRC2-SP3	RCM/*i,i* + 4 position	39	None	[73]
	5DXE	SRC2-SP4	RCM/*i,i* + 4 position	–	None	[73]
	5DXG	SRC2-SP5	–	–	–	[73]
	5WGD	SRC2-LP1	RCM/*i,i* + 4 position	–	Hydrophobic contacts between ILe689 and Leu693 with the hydrophobic shelf of ER_{α}	[74]
	5WGQ	SRC2-BCP1	Cross stitch (olefin & lactam)/orthogonal position	–	Sub-optimal hydrophobic interaction	[74]
Aurora-A	5LXM	Stapled TPX2 peptide 10	RCM/*i,i* + 4 position	0.18 μM	None	[73]
Tankyrase 2	5BXO	Cp4n2m3	Double-click Cycloaddition reaction/*i,i* + 4 position	0.6 ± 0.01 μM	None	[55]
	5BXU	Cp4n4m5	Double-click Cycloaddition reaction/*i,i* + 4 position	2.8 ± 0.1 μM	None	[55]
Grb7	5D0J	G7-B4NS peptide	RCM+ Thioether/monocyclic peptide	4.93 ± 0.03 μM	None	[56]
	5EEL	G7-B4 peptide	RCM+ Thioether/bicyclic peptide	0.83 ± 0.006 μM	Close contacts with Met495, Asp496, Asp497 backbone and sidechains of EF loop of Grb7-SH2 and Ile 518 of BG loop	[56]
	5EEQ	G7-B1 peptide	RCM+ Thioether/bicyclic peptide	1.5 ± 0.01 μM	Close contacts with Met495, Asp496, Asp497 backbone and sidechains of EF loop of Grb7-SH2 and Ile 518 of BG loop	[56]
Replication protein A	4NB3	Peptide-33	–	0.022 ± 0.005 μM	–	[75]
eIF4E	4BEA	sTIP-04 Stapled peptide	RCM/*i,i* + 4 position	FP/11.5 ± 3.6 SPR/5 ± 0.7	None	[58]
β-catenin	4DJS	aStAx-35	RCM/*i,i* + 4 position	13 ± 2.0	None	[76]
hDcn-1	3TDZ	$hCul1^{WHB}$: $hDcn1^{P}$: Acetyl-$hUbc12^{1-12}$ (5:9 Staple)	RCM/*i,i* + 4 position	0.15 μM	None	[77]
Insulin	3KQ6	[$HisA^4$, $HisA^8$] insulin	–	IGF-1R/0.05 ± 0.01 IR/125 ± 18	–	[54] [52]
ks-vFLIP	5LDE	spIKKγ-Stapled peptide	RCM/*i,i* + 4 position	30.4 ± 3.8 μM	None	[59]
TLE1	5MWJ	Peptide18	RCM/*i,i* + 4 position	522 ± 39.6	None	[57]
Human IgG1 Fc	5U66	LH1	RCM/*i,i* + 7 position	~1 ± 0.5 mM	None	[78]
Ca_V β subunit	5V2P	AID-CAP Stapled peptide	*m-xyl*yl linker macrocyclization/*i,i* + 5 position	5.1 ± 1.6	None	[78]
Ca_V β subunit	5V2Q	AID-CEN Stapled peptide	*m-xyl*yl linker macrocyclization/*i,i* + 4 position	5.2 ± 1.5	None	[75]

(continued on next page)

Table 3 (*continued*)

Target	PDB ID	Peptide	Cyclisation Method	K_d (nM)	Staple Interaction	Ref.
Target	PDB ID	Peptide	Cyclisation Method	K_d (nM)	Staple Interaction	Ref.
NCOA1	5Y7W	YL-2	RCM/*i*,*i* + 4 position	–	None	[79]
Saccharomycs cerevisiae	5NXQ	Sld5 CIP A2	Double-click Cycloaddition reaction (CuAAC)/*i*,*i* + 6 position	0.32 ± 0.02 μM	None	[80]
	4HU6	GCN4-p1(7b)	Oxime bridge (covalent cross-link)/*i*,*i* + 4 position	–	Internal polar contact between Gln4 and the U5 carbonyl of the oxime bridge.	[81]
HIV-1	4NGH	SAH- MPER $_{(671\text{-}683KKK)}$(q)pSer	RCM/*i*,*i* + 4 position (R3-S5)	–	None	[13]
	4NHC	SAH-MPER$_{(671\text{-}683KKK)}$ (q)	RCM/*i*,*i* + 4 position (R3-S5)	–	None	[13]
	4U6G	SAH-MPER$_{(662\text{-}683KKK)}$ (B,q)	RCM/*i*,*i* + 4 position (R3-S5)		None	[13]
Plasmodium falciparum	4MZJ	pGly[801–805]	RCM/*i*,*i* + 4 position	–	Hydrophobic contact with Trp171 and Asp173	[90]
	4MZK	pGly[807-811]	RCM/*i*,*i* + 4 position	–	Hydrophobic contact with Phe148, Leu168, Leu175 an Ile202	[90]
Synthetic collagen	3P46	SS1	Double-click Cycloaddition reaction (CuAAC) 2 + 1 strand click-reaction/C-terminal	–	None	[93]
EphA2-Sam/Ship2-Sam complex	6F7M	S13ST	RCM/*i*,*i* + 4 position	Ship2-Sam/52.2 ± 0.7 μM	None	[94]
Human Cul3-BTB	2MYL	Cul3$^{49\text{-}68EN}$	RCM/*i*,*i* + 4 position	620 ± 177	None	[95]
	2MYM	Cul3$^{49\text{-}68LA}$	RCM/*i*,*i* + 4 position	305 ± 100	None	[95]
De novo proteins	2M7C	Cp-T^{2}C3b	Gly-Gly linker	–	None	[98]
	2M7D	(P12W)-T^{2}C16b	Gly-Gly linker	–	None	[98]

conformation, a coactivator protein binding-groove is formed, conversely in the antagonist-bound conformation; the groove is lost. The co-activator binding-site is mediated by a short leucine-rich pentapeptide, with the amino acid consensus sequence LXXXLL, known as the NR box. This peptide was found to form amphipathic α-helices, in which the three conserved leucine residues are on the hydrophobic face that binds to the coactivator-binding groove. On the other side of the binding site, the receptor surface has charged recognition residues that bind to the N and C-terminus of the helix, known as a charge clamp. Modeling of peptide inhibitors that bind to ER and work allosterically could create a new class of NR-regulating drugs. Phillips and his group [72] designed and synthesized a series of these peptides, aiming to bind and inhibit ER as pharmacological candidates. Two stapled peptides known as SP1 and SP2 showed increased helicity as judged by CD. SP1 showed ~4 fold stronger binding to ER when compared to unstapled peptides with a K_d of 1.99 μM, while SP2 peptide gave 2-fold increase in binding relative to SP1 (K_d of 352 nM), as determined by an SPR assay. The binding mode of both peptides followed

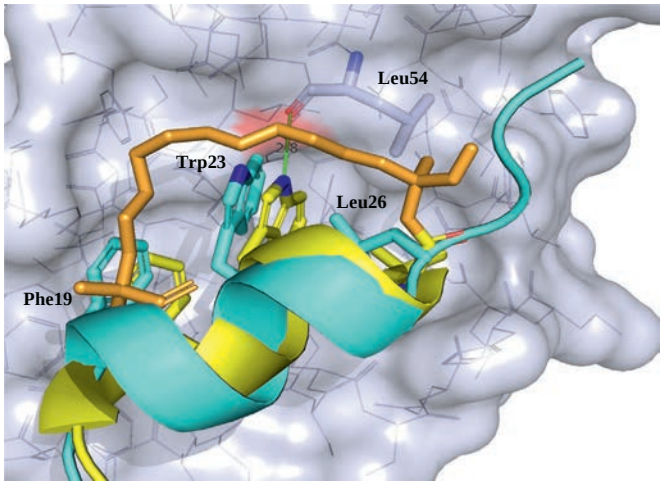

Fig. 11. Alignment of the SAH-p53-8 peptide (yellow, PDB 3V3B) and the native p53 peptide (cyan, PDB 1YCR). The MDM2 molecule is shown in surface representation. SAH-p53-8 peptide mimics the three pharmacophore residues (Phe19, Leu26, Trp23) in the binding site in a similar manner to the native p53. The residues outside the Phe19-Leu26 regions are not visible, indicating conformational flexibility in the bound state. Moreover, the whole helix of stapled peptide moves by ~1 Å and is rotated by 18°, allowing the Trp23 indole ring to form a hydrogen bond with MDM2 Leu54 (green line). Interestingly, Leu26 orientates itself in a distinct manner to that of the native p53 ^{Leu26}, (moving by 2.7 Å toward the N-terminus of the peptide) and the side chain is flipped by approximately 180° to fill the same pocket space. This feature is not found in any other reported structure. (For interpretation of the references to color in this figure legend, the reader is referred to the web version of this article.)

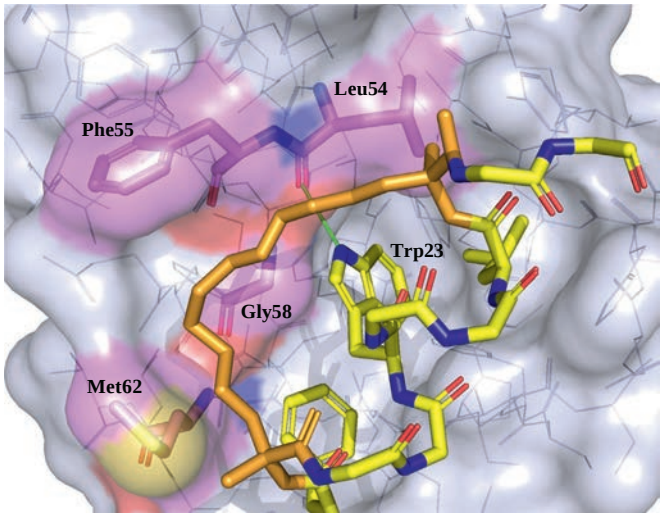

Fig. 12. A closer view of the SAH-p53-8 stapled peptide in a "closed" conformation state. The MDM2 molecule is shown in surface representation, the peptide (yellow) and the staple (orange) in sticks. A hydrogen bond is formed between the indole nitrogen atom of the peptide helix and the carbonyl oxygen of Leu54 of MDM2 (green line). This H-bound is protected from solvent competition by the staple that lied directly over Met50-Lys64 helix (the rim of p53 binding site). In addition, the staple intimately interacts with the protein surface and forms an extended hydrophobic interface with Leu54, Phe55, Gly58, and Met62 of Mdm2. (For interpretation of the references to colour in this figure legend, the reader is referred to the web version of this article.)

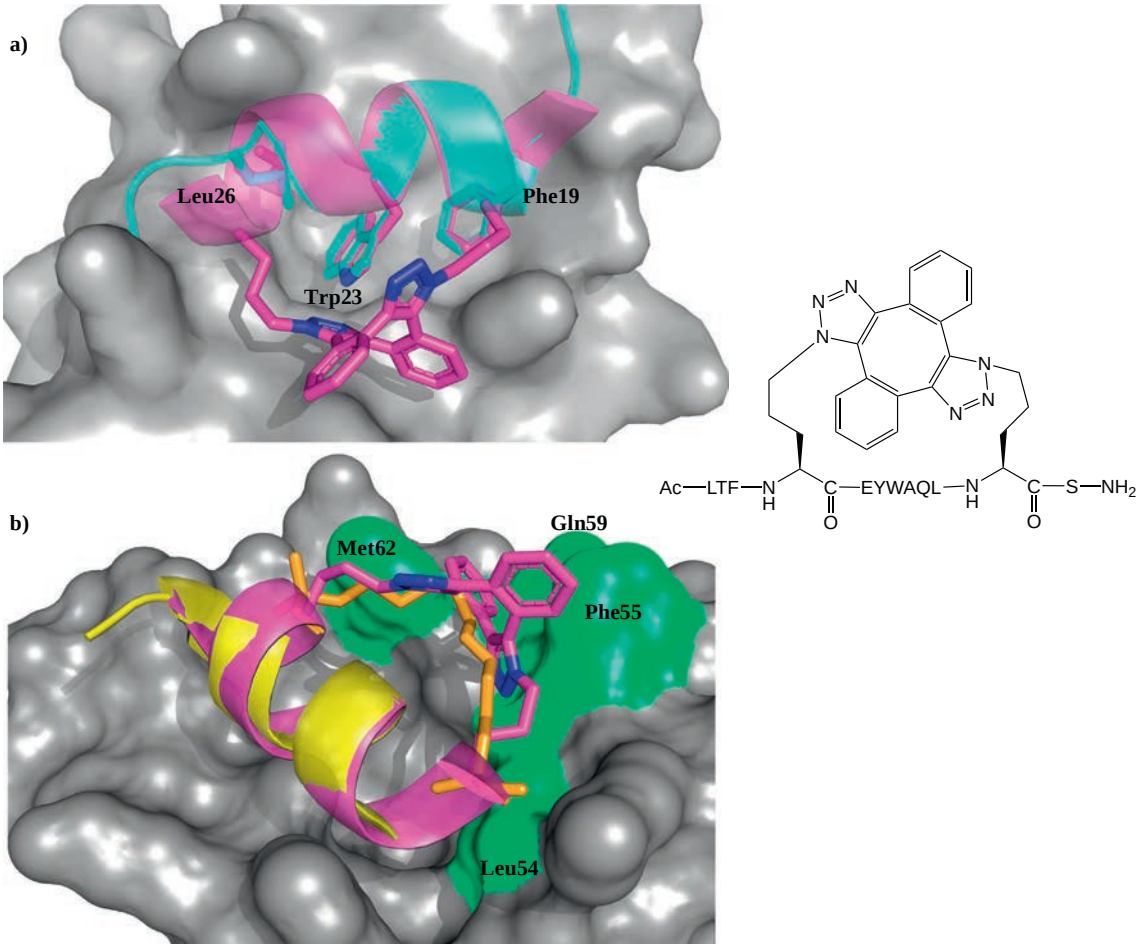

Fig. 13. The E1-MDM2 complex high-resolution structure at 1.9 Å. a) top view of E1 stapled peptide (magenta, PDB 5AFG) aligned with the native peptide p53 (cyan, PDB 1YCR), revealing the typical mode of binding within the MDM2 hydrophobic pocket (grey surface) - placing the triad residues responsible for binding (P2he19, Trp23, Leu26) in the correct orientation to engage the MDM2 hotspots. The staple is found in *anti* regioisomer form and interacts with protein surface a similar mode as b) previously reported hydrocarbon SAH-p53-8 stapled peptide (PDB 3V3B), in that the stapled form four hydrophobic interactions with MDM2 surface residues (Leu54, Phe55, Gln59 and Met62, lime green), in which Phe55 is the most critical residue. The superimposition of the triazole-stapled E1 peptide with the correlated hydrocarbon-stapled p53 peptide (yellow, PDB 3V3B) suggests that both staples engage the same area that is located at the rim of the p53 binding pocket, on the Met50–Lys64 helix. The E1 stapled peptide is also shown in 2D for clarity (right). (For interpretation of the references to colour in this figure legend, the reader is referred to the web version of this article.)

the same manner within the co-activator binding-site as shown by high-resolution structures at 1.9 Å for SP1 ERβ structure (PDB 1YJD), and 1.8 Å for the SP2 ERα structure (PDB 2YJA). The conserved NR box LXXLL recognition motif was replaced with the IXXS5L motif in SP1; as expected the recognition site does not bind in the groove. Alternatively, the *i,i + 4* hydrocarbon staple "at S5 position of the motif" was linked to the SP1 helix by RCM, which made comprehensive van der Waals contacts with the hydrophobic residues Val307, Ile310, and Leu490 of the co-activator protein binding groove (Fig. 16). As in the SP1 ERβ structure, the same interactions for the staple with the hydrophobic groove of the coactivator site were found in the SP2 ERα structure (Fig. 16). The reported structures demonstrate the importance of designing stapled peptides that inhibit NRs and PPIs in which stapling not only reinforces the helix conformational but also promotes staple interaction with the hydrophobic surface of the target protein. Together this makes stapled peptides promising therapeutic targets, even for the undruggable targets of traditional small-molecule inhibitors. A comparison analysis between the stapled peptides SP1, SP2 and an earlier reported NR co-activator peptide 2 in complex with ERα (PDB 2QGT) revealed a quarter turn of the SP1 helix that shifts the binding site residues by one position in the reference recognition site (Fig. 17a). However, the SP2 stapled peptide showed conformational changes of Asp538 and Ile358 residues on the receptor site in contrast to the co-activator peptide 2. In SP2 residue Asp538 rotates in toward the peptide, while it moves out in the co-activator peptide structure to adjust the Ile side chain into the peptide-binding motif. Furthermore, Ile358 of the SP2 peptide adopts a distinct rotamer and packed closer than the second Leu of the coactivator peptide 2, which in turn allows the staple to span over the C-terminal recognition motif with a 100° rotation toward the other side of the protein IL__LL contact site (Fig. 17b).

5. Computational Approach for Staple Peptide Design

Hydrocarbon stapled peptides are at a relatively early stage of development. Over the last decade important information about the effects of staple position, staple structure, and peptide sequence on the activity of stapled peptides have become available [65]. Most of the reported stapled peptides in the literature have classically been designed based either on previous high-resolution structures or comprehensive alanine scanning studies [5,112]. On the other hand, staple positioning is usually optimized via chemical synthesis and biophysical characterization of every possible variant of a peptide construct. However, these methods are by no means comprehensive and provide little insight about the behavior of a stapled construct in living cells [113]. Moreover, experimental characterization of the stapled peptides is neither economically viable nor feasible within a reasonable timeline, especially for long peptides, and is considered tedious and expensive [65,113].

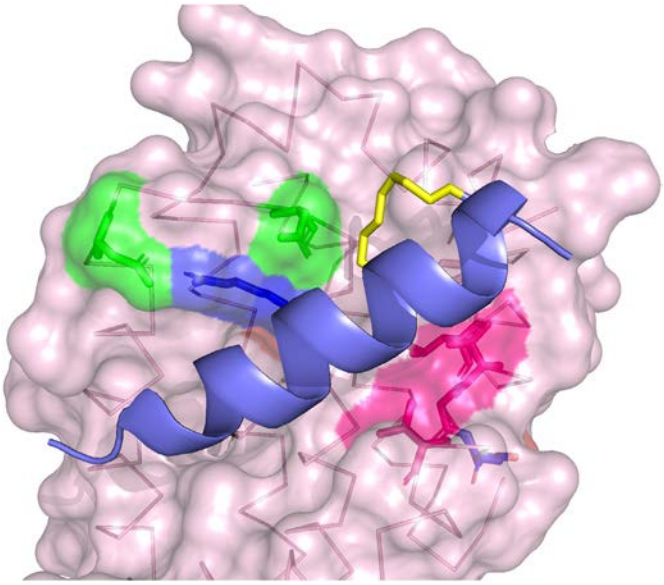

Fig. 14. The crystal structure of MCL-1 $SAHB_D$ stapled peptide (slate helix) binding to the MCL-1ΔNΔC (light pink surface) interface at the canonical BH3-binding groove, solved at 2.3 Å resolution (PDB 3MK8). The peptide makes several hydrophobic interactions, including the hydrophobic residues Leu213, Val216, Gly217, and Val220 of MCL-1 $SAHB_D$ making direct contact with a hydrophobic cleft at the surface of MCL- 1ΔNΔC (hot pink). The hydrophobic interaction are reinforced by a salt bridge between MCL-1 $SAHB_D$ Asp218 and MCL-1ΔNΔC Arg263 (blue) and these residues also contribute to a hydrogen bond cluster that includes MCL-1ΔNΔC Asp256 and Asn260 (green). (For interpretation of the references to colour in this figure legend, the reader is referred to the web version of this article.)

As a result, computational tools have become an essential part of the stapled peptide design process, because they help to rationalize practical/experimental observations, provide insight into molecular mechanisms of binding, and identify promising candidate peptides, thus reducing the need for extensive screening of peptide libraries. At the same time, utilizing allows to efficiently build and characterize peptide candidates *in silico*. Thus, we are able to explore each possible staple location along the peptide backbone in order to ensure that each candidate is considered in the search. All of these advantages reduce costs and time that are necessary to design and optimize the lead stapled peptide for detailed experimental studies [65,113].

Several computational methods or techniques have been employed in stapled peptide design, including Energy minimization, Monte Carlo (MC) simulation and Molecular dynamics (MD) [65].

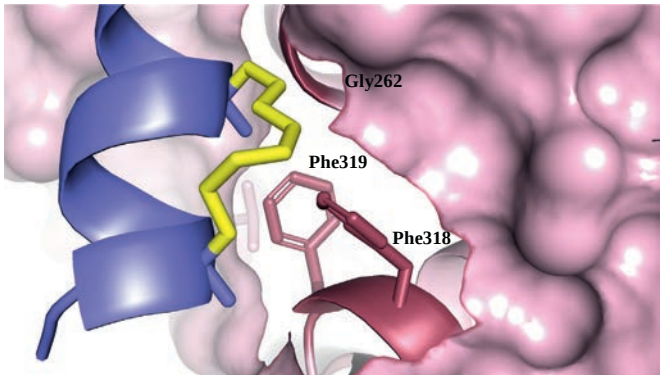

Fig. 15. The hydrocarbon staple of MCL-1 $SAHB_D$ peptide with an alkene functionality in the *cis* conformation (yellow stick) makes distinct hydrophobic contacts with the MCL-1ΔNΔC binding site border (light pink surface). A methyl group of the α,α-dimethyl functionality engages with a groove consisting of MCL-1ΔNΔC Gly262, Phe318, and Phe319 residues (raspberry sticks). (For interpretation of the references to colour in this figure legend, the reader is referred to the web version of this article.)

An example of a successful computational approach was the CCmut3 stapled peptide, a Bcr-Abl kinase agonist that effectively reduces the oncogenic potential of Bcr-Abl. By applying different *in silico* tools such as Chimera [114], AmberTools15 [115] and hydrogen mass repartitioning (HMR) for accelerating molecular dynamics (MD) simulations [113,116]; the authors were able to explore 64 peptide analogues with different possible positions of staple along peptide backbone. Such models can be used to characterize a wider range of possibilities than was possible experimentally, due to CCmut3 peptide length, which is considered long. Additionally, the length of the peptide introduces a high degree of conformational variability and opportunity to be targeted by intracellular proteolytic mechanisms. The authors concluded that computational methods can play a key role in the design process of therapeutics peptides, specifically in exploring an exceptionally large and diverse set of candidates in a short timeframe compared to experimental settings [113].

6. Conclusion

Inhibiting protein-protein interactions (PPI) has become a general strategy for interpreting the molecular logic associated with PPI networks, or for therapeutic applications. The later approach was explored extensively over the last ten years by introducing a new class of targeted inhibitors known as hydrocarbon-stapled peptides. Peptides originating from livestock and biological sources have low stability, short half-life and unstable secondary-structures due to their sensitivity toward proteolysis [1,16]. These impact peptide bioavailability and binding to their intracellular target interfaces, making peptides a poor drug candidate. However, small molecules are successful drug candidates due to their size, oral bioavailability and cell penetration. In addition, small molecules are more appropriate for small and compact protein interfaces with a size range of 300–1000 Å [8] such as, BCL2 & BCL-xL proteins (Fig. 18a) [117], p53-MDM2 (Fig. 18b) [62,118] and Hsp90 [119,120] (Fig. 18c). Selected examples of these fruitful small-molecules drugs are *Obatoclax* (GS-01570) which entered Phase II clinical trials in patients with small-cell lung cancer [121–124]; *Nutlin* and its derivatives [125] led to the evolution of *RG7112* as a first MDM2 inhibitor that entered clinical trials in advanced solid tumor patients in 2007. This was followed by *RO5503781* that entered Phase I clinical trials in patients with advanced malignancies in 2011 and ended in 2014 (https://clinicaltrials.gov/ct2/show/record/NCT01462175). A last example is a natural product (*Geldanamycin (GM)* (Fig. 18c)), which was the first molecule to inhibit Hsp90. *Geldanamycin* entered clinical trials and its clinical derivative, *17-AAG*, reached phases I and II trials in patients with multiple myeloma, lymphoma, stage IV pancreatic cancer, non-small-cell lung cancer and solid tumors [126].

Despite the success of small-molecules to perturb different PPIs, these traditional inhibitors are not sufficient to cover large interfaces, which are more likely amenable to peptidomimetics. Subsequently, synthetic and medicinal chemistry developments delivered stapling as a technique to overcome the limitation of native peptides in stability, resistance to proteolysis degradation, specificity to targets and cell penetration. Depending on the size of the targeted interface, the affinity of the interaction and the position of hot spots residues, different strategies have been generated to synthesize stapled peptides targeting major PPIs interfaces of previously undruggable protein networks. All-hydrocarbon stapled peptides lead to the discovery of new candidate drugs, combining the advantages of small-molecules and biologics. Examples of these interfaces are p53-MDM2/MDMX, BCL-2 family including MCL-1 BH3 domain, Estrogen receptor, Human immunodeficiency virus type 1 (HIV-1), kinases and Growth factor. As a result, stapling has found a unique therapeutic niche as an important class in the pharmaceutical field. Furthermore, scientific technology innovation and novel chemistry methodologies broaden therapeutic peptide diversity and improve their

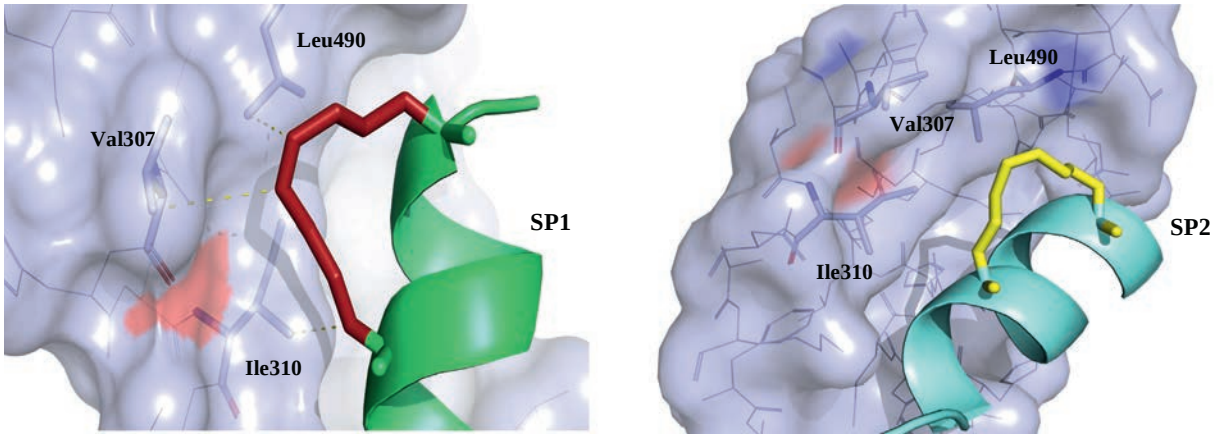

Fig. 16. The crystal structures of the SP1 ERβ (PDB 1YJD) and SP2 ERα (PDB 2YJA) complexes at 1.9 and 1.8 Å resolution, respectively. Van der Waal interactions (yellow dash lines) were found between both staples of SP1 and SP2 peptides and the hydrophobic residues on the surface of the co-activator binding site Val307, Ile310 and Leu490. ERβ and ERα proteins are shown in surface representation, while the staple of the both peptides and the interacting residues are in sticks. (For interpretation of the references to colour in this figure legend, the reader is referred to the web version of this article.)

pharmaceutical properties. In addition, advances in peptide screening and computational biology will continue to support peptide drug discovery. It has been found that stapling increased peptide helicity and reinforces the α-helix confirmation as shown in several studies, as well as enhancing specificity and binding affinity to the targeted protein interface [58,62,65,68,71]. However, some obstacles need to be overcome to improve therapeutic properties, such as cellular penetration. In this case, new peptide drug delivery and formulation approaches are necessary for this unique class of drugs, although some peptides show high permeability by endocytosis by optimizing helicity %, PI and hydrophobicity together [127]. Consequently, future studies should focus on the factors that promote cellular uptake and endosomal release in stapled peptide design. Another challenge that must be overcome is the oral availability of peptide therapeutics, which could be boosted by increasing drug stability in the gastrointestinal tract, again by formulating peptide penetration with enhancers or congregating with carrier molecules or nanoparticles [128–130]. Finally, in some cases, stapled peptides with high affinities do not necessary translate to the target cell, as Wallbrecher and Okamoto demonstrated when applying stapling to BimBH3 peptides to bind BCL-2 proteins and induce apoptosis [131,132]. In agreement, PPI antagonists are usually evaluated using *in vitro* biochemical and biophysical assays like fluorescence polarization (FP), surface plasmon resonance (SPR) [25,29,133], isothermal calorimetry (ITC) [32], enzyme-linked immunosorbent assay (ELIZA) [134] and fluorescence or bioluminescence resonance excitation transfer (FRET/BRET) [135,136] to quantify their binding potency and ability to disrupt the targeted PPI. Even with the availability of fluorescent image-based assays such as the proximity ligation *in situ* assay (P-LISA) [137,138] and two/three hybrid (F2H and F3H) assays [99,139] to assess PPI antagonists in real-time within the cells; none can reveal whether these antagonists can cross the cell membrane effectively in a native intracellular environment. To overcome this issue, the ReBiL platform has been developed by Li and co-workers to detect weak PPI interactions and mechanisms of drug action in living cells. It has been successfully applied on antagonists of p53:

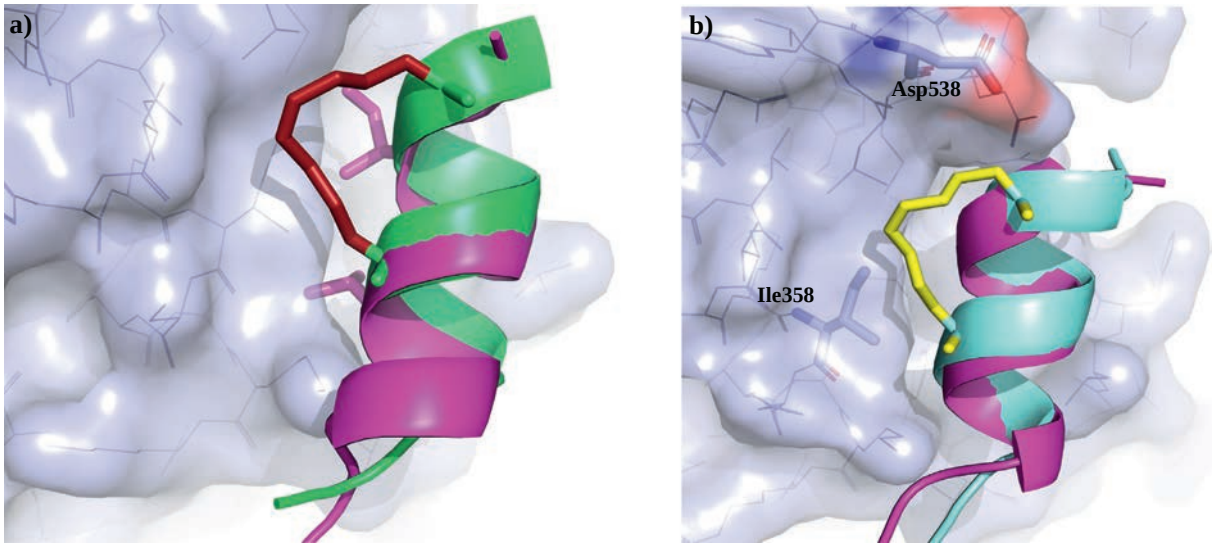

Fig. 17. Comparison analysis of a) SP1 (lime green helix) and b) SP2 (aquamarine helix) stapled peptides in relation to previously reported NR co-activator peptide 2 (light magenta helix, PDB 2QGT). a) SP1 stapled peptide exhibited a quarter turn with respect to the co-activator peptide locating the hydrophobic staple to the recognition site position. While b) SP2 rotates differently and packs tighter than the coactivator peptide 2 does. Additionally, two residues in the receptor site (Asp538 and Ile358) induce conformational changes bridging the staple of SP2 helix to the C-terminus site of the recognition motif that is rotated by 100° toward the other side of the protein IL__LL contact site. (For interpretation of the references to colour in this figure legend, the reader is referred to the web version of this article.)

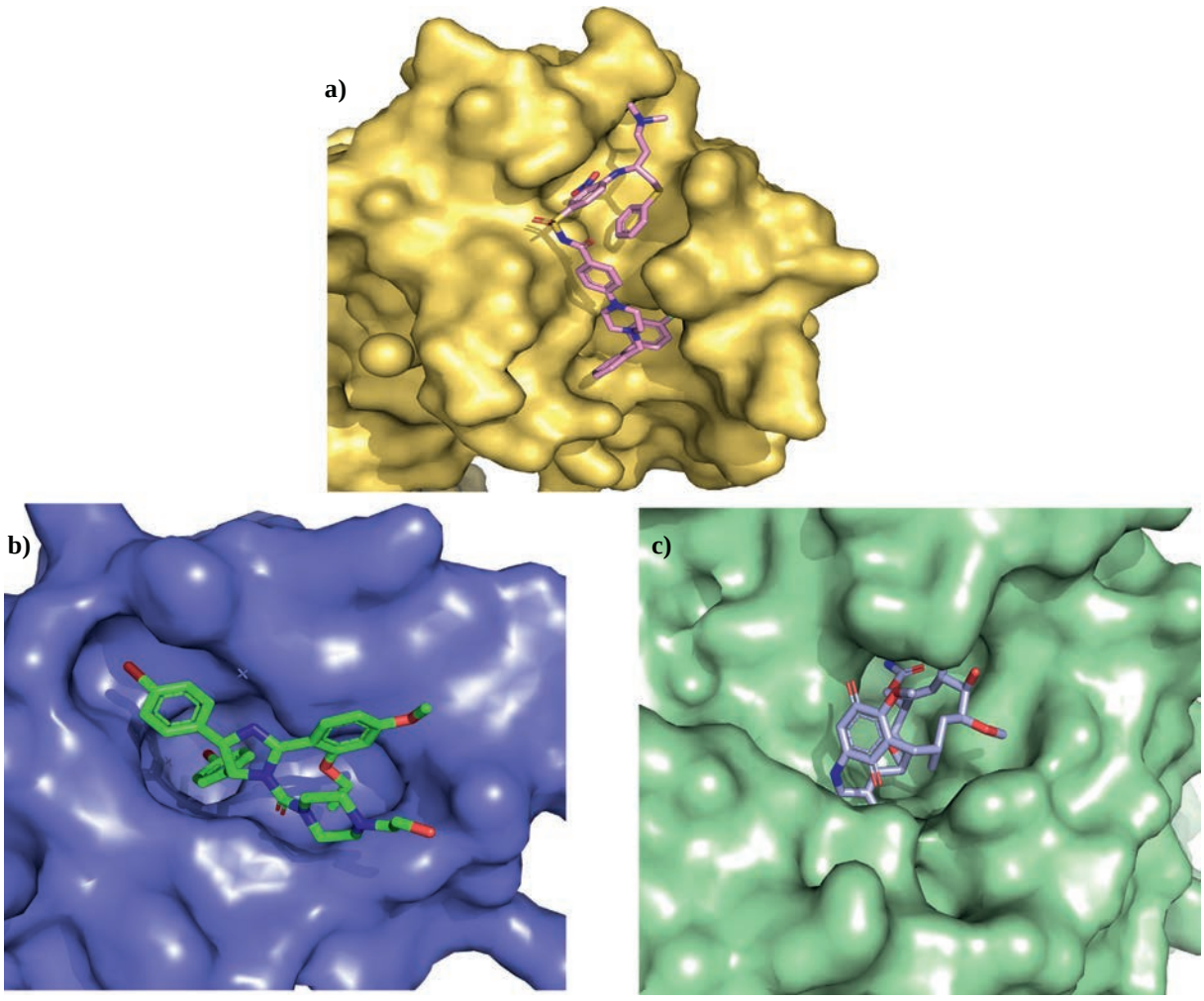

Fig. 18. Crystal structures of successful small molecules inhibiting drug-target PPIs that have entered clinical trials. a) ABT-737 (pink sticks) binds to BCL-xL (PDB 2YXJ) with nanomolar binding affinity, b) Nutlin-2 (green sticks), is one of the first identified potent MDM2–p53 inhibitors and is shown bound to the N-terminal domain of MDM2 (PDB 1RV1) and c) geldanamycin (GM) (light blue stick) in complex with Hsp90 (PDB 1YET), considered the first Hsp90 inhibitor to enter clinical trials. (For interpretation of the references to colour in this figure legend, the reader is referred to the web version of this article.)

MDM2 PPI, including small molecule Nutlin-3a and three stapled peptides (SAHBp53-8, ATSB-7104 and sMTide-02). They revealed that potent binding *in vitro* does not necessarily correlate with higher intracellular PPI disruption activity. This emphasizes the importance of using an assay like ReBiL to analyze directly the disruption of target PPI within cells [140].

Interestingly, relatively few reported high-resolution structures of stapled peptide in complex with their target interface reveal a direct interaction between the staple itself and residues of the protein interfaces (Table 2). A phenomenon is observed with the MCL-1 $SAHB_D$/MCL-1, SAH-p53-8/MDM2, E1/MDM2, SP1/ERβ and SP2/ERα complexes, in which staples make additional hydrophobic interaction with protein surface residues that fix the peptide in a bound state within the target pocket. Additionally, the staple can play a role in peptide penetration and bioactivity [127].

Taken together, hydrocarbon-stapled peptides are a fertile ground for drug discovery. However, the development of highly cell-permeable and bioactive peptides is a challenging task that includes several phases. Starting from the correct design of the peptide, screening of different stapling positions and/or point mutations, measuring binding affinities and testing specificity toward the target protein interface, structural and computational analysis should be performed in order to understand how the peptide and/or staple binds and which interactions are involved. Importantly, two questions need to be tackled in current research: Firstly, can a stapled peptide with significant *in vitro* results penetrate the cell membrane toward the target PPI complex? Secondly, if it reaches the target PPI, will this peptide exert the expected bioactivity *in vivo*? This question could be addressed with future research aiming to tailored bioactive therapeutic peptides with high permeability and increased precision to PPIs within the targeted cell using advanced medicinal and synthetic chemistry in parallel with computational and drug delivery approaches.

Acknowledgment

This research has been supported to (AD) by the National Institute of Health (NIH) (2R01GM097082-05), the European Lead Factory (IMI) under grant agreement number 115489, the Qatar National Research Foundation (NPRP6-065-3-012). Moreover funding was received through ITN “Accelerated Early stage drug dIScovery” (AEGIS, grant agreement No 675555) and, COFUND ALERT (grant agreement No 665250) and KWF Kankerbestrijding grant (grant agreement No 10504). A.A was supported by Qatar leadership program, Qatar foundation.

References

[1] Craik DJ, Fairlie DP, Liras S, Price D. The future of peptide-based drugs. Chem Biol Drug Des 2013;81:136–47. https://doi.org/10.1111/cbdd.12055.

[2] Rosenblum D, Peer D. Omics-based nanomedicine: the future of personalized oncology. Cancer Lett 2014;352:126–36. https://doi.org/10.1016/j.canlet.2013.07.029.

[3] Ruffner H, Bauer A, Bouwmeester T. Human protein–protein interaction networks and the value for drug discovery. Drug Discov Today 2007;12:709–16. https://doi.org/10.1016/J.DRUDIS.2007.07.011.

[4] Yan C, Wu F, Jernigan RL, Dobbs D, Honavar V. Characterization of protein-protein interfaces. Protein J 2008;27:59–70. https://doi.org/10.1007/s10930-007-9108-x.

[5] Verdine GL, Hilinski GJ. Stapled peptides for intracellular drug targets. . 1st ed., vol. 503Elsevier Inc; 2012. https://doi.org/10.1016/B978-0-12-396962-0.00001-X.

[6] Pérot S, Sperandio O, Miteva MA, Camproux AC, Villoutreix BO. Druggable pockets and binding site centric chemical space: a paradigm shift in drug discovery. Drug Discov Today 2010;15:656–67. https://doi.org/10.1016/j.drudis.2010.05.015.

[7] Ivanov AA, Khuri FR, Fu H. Targeting protein-protein interactions as an anticancer strategy. Trends Pharmacol Sci 2013;34:393–400. https://doi.org/10.1016/j.tips.2013.04.007.

[8] Smith MC, Gestwicki JE. Features of protein–protein interactions that translate into potent inhibitors: topology, surface area and affinity. Expert Rev Mol Med 2012;14:e16. https://doi.org/10.1017/erm.2012.10.

[9] Fang Z, Song Y, Zhan P, Zhang Q, Liu X. Conformational restriction: an effective tactic in 'follow-on'-based drug discovery. Future Med Chem 2014;6:885–901. https://doi.org/10.4155/fmc.14.50.

[10] Gilson MK, Zhou H-X. Calculation of protein-ligand binding affinities. Annu Rev Biophys Biomol Struct 2007;36:21–42. https://doi.org/10.1146/annurev.biophys.36.040306.132550.

[11] Bakail M, Ochsenbein F. Targeting protein-protein interactions, a wide open field for drug design. C R Chim 2016;19:19–27. https://doi.org/10.1016/j.crci.2015.12.004.

[12] Okamoto T, Segal D, Zobel K, Fedorova A, Yang H, Fairbrother WJ, et al. Further insights into the effects of pre-organizing the BimBH3 Helix. ACS Chem Biol 2014;9:838–9. https://doi.org/10.1021/cb400638p.

[13] Bird GH, Irimia A, Ofek G, Kwong PD, Wilson IA, Walensky LD. Stapled HIV-1 peptides recapitulate antigenic structures and engage broadly neutralizing antibodies. Nat Struct Mol Biol 2014;21:1058–67. https://doi.org/10.1038/nsmb.2922.

[14] Lau YH, De Andrade P, Wu Y, Spring DR. Peptide stapling techniques based on different macrocyclisation chemistries. Chem Soc Rev 2015;44:91–102. https://doi.org/10.1039/c4cs00246f.

[15] Jenssen H, Aspmo SI. Serum stability of peptides. Methods Mol Biol 2008;494:177–86. https://doi.org/10.1007/978-1-59745-419-3_10.

[16] Tsomaia N. Peptide therapeutics: targeting the undruggable space. Eur J Med Chem 2015;94:459–70. https://doi.org/10.1016/j.ejmech.2015.01.014.

[17] Jubb H, Higueruelo AP, Winter A, Blundell TL. Structural biology and drug discovery for protein-protein interactions. Trends Pharmacol Sci 2012;33:241–8. https://doi.org/10.1016/j.tips.2012.03.006.

[18] Lau JL, Dunn MK. Therapeutic peptides: historical perspectives, current development trends, and future directions. Bioorg Med Chem 2018;26:2700–7. https://doi.org/10.1016/j.bmc.2017.06.052.

[19] Schafmeister CE, Po J, Verdine GL. An all-hydrocarbon cross-linking system for enhancing the helicity and metabolic stability of peptides [8]. J Am Chem Soc 2000;122:5891–2. https://doi.org/10.1021/ja000563a.

[20] Tyndall JDA, Nall T, Fairlie DP. Proteases universally recognize beta strands in their active sites, vol. 105; 2005; 973–1000. https://doi.org/10.1021/cr040669e.

[21] Nowick JS. Exploring β-sheet structure and interactions with chemical model systems. Acc Chem Res 2008;41:1319–30. https://doi.org/10.1021/ar800064f.

[22] Harrison RS, Shepherd NE, Hoang HN, Ruiz-Gomez G, Hill TA, Driver RW, et al. Downsizing human, bacterial, and viral proteins to short water-stable alpha helices that maintain biological potency. Proc Natl Acad Sci 2010;107:11686–91. https://doi.org/10.1073/pnas.1002498107.

[23] Kim Y-W, Grossmann TN, Verdine GL. Synthesis of all-hydrocarbon stapled α-helical peptides by ring-closing olefin metathesis. Nat Protoc 2011;6:761–71. https://doi.org/10.1038/nprot.2011.324.

[24] Blackwell HE, Grubbs RH. Highly efficient synthesis of covalently cross-linked peptide helices by ring-closing metathesis. Angew Chem Int Ed 1998;37:3281–4. https://doi.org/10.1002/(SICI)1521-3773(19981217)37:23<3281::AID-ANIE3281>3.0.CO;2-V.

[25] Walensky LD, Kung AL, Escher I, Malia TJ, Barbuto S, Wright RD, et al. Activation of apoptosis in vivo by a hydrocarbon-stapled BH3 helix. Science 2004;305. https://doi.org/10.1126/SCIENCE.1099191 80-. 1466–70.

[26] Ahrens VM, Bellmann-Sickert K, Beck-Sickinger AG. Peptides and peptide conjugates: therapeutics on the upward path. Future Med Chem 2012;4:1567–86. https://doi.org/10.4155/fmc.12.76.

[27] Miller MJ, Foy KC, Kaumaya PTP. Cancer immunotherapy: present status, future perspective, and a new paradigm of peptide immunotherapeutics. Discov Med 2013;15(82):166–76.

[28] Vlieghe P, Lisowski V, Martinez J, Khrestchatisky M. Synthetic therapeutic peptides: science and market. Drug Discov Today 2010;15:40–56. https://doi.org/10.1016/J.DRUDIS.2009.10.009.

[29] Bernal F, Tyler AF, Korsmeyer SJ, Walensky LD, Verdine GL. Reactivation of the p53 tumor suppressor pathway by a stapled p53 peptide. J Am Chem Soc 2007;129:2456–7. https://doi.org/10.1021/ja0693587.

[30] Bird GH, Madani N, Perry AF, Princiotto AM, Supko JG, He X, et al. Hydrocarbon double-stapling remedies the proteolytic instability of a lengthy peptide therapeutic. Proc Natl Acad Sci 2010;107:14093–8. https://doi.org/10.1073/pnas.1002713107.

[31] Bird GH, Christian Crannell W, Walensky LD. Chemical synthesis of hydrocarbon-stapled peptides for protein interaction research and therapeutic targeting. Curr Protoc Chem Biol 2011;3:99–117. https://doi.org/10.1002/9780470559277.ch110042.

[32] Walensky LD, Bird GH. Hydrocarbon-stapled peptides: principles, practice, and progress. J Med Chem 2014;57:6275–88. https://doi.org/10.1021/jm4011675.

[33] Wang Y, Chou DH. A thiol – Ene coupling approach to native peptide stapling and macrocyclization ** Angewandte. Angew Chem Int Ed 2015;54:10931–4. https://doi.org/10.1002/anie.201503975.

[34] Kneissl S, Loveridge EJ, Williams C, Crump MP, Allemann RK. Photocontrollable peptide-based switches target the anti-apoptotic protein Bcl-x_L. Chem Bio Chem 2008;9:3046–54. https://doi.org/10.1002/cbic.200800502.

[35] Chang YS, Graves B, Guerlavais V, Tovar C, Packman K, To K-H, et al. Stapled α−helical peptide drug development: a potent dual inhibitor of MDM2 and MDMX for p53-dependent cancer therapy. Proc Natl Acad Sci 2013;110:E3445–54. https://doi.org/10.1073/pnas.1303002110.

[36] Hilinski GJ, Kim Y-W, Hong J, Kutchukian PS, Crenshaw CM, Berkovitch SS, et al. Stitched α-helical peptides via bis ring-closing metathesis; 2014. https://doi.org/10.1021/ja505141j.

[37] Felix AM, Heimer EP, Wang CT, Lambros TJ, Fournier A, Mowles TF, et al. Synthesis, biological activity and conformational analysis of cyclic GRF analogs. Int J Pept Protein Res 1988;32:441–54. https://doi.org/10.1111/j.1399-3011.1988.tb01375.x.

[38] Greenfield N, Fasman GD. Computed circular dichroism spectra for the evaluation of protein conformation. Biochemistry 1969;8:4180–4116. doi:https://doi.org/10.1021/bi00838a031.

[39] Shepherd NE, Hoang HN, Abbenante G, Fairlie DP. Single turn peptide alpha helices with exceptional stability in water. J Am Chem Soc 2005;127:2974–83. https://doi.org/10.1021/ja0456003.

[40] Khoo KK, Wilson MJ, Smith BJ, Zhang M-M, Gulyas J, Yoshikami D, et al. Lactam-stabilized helical analogues of the analgesic μ-conotoxin KIIIA. J Med Chem 2011;54:7558. https://doi.org/10.1021/JM200839A.

[41] Moses JE, Moorhouse AD, Kolb HC, Finn MG, Sharpless KB, Kolb HC, et al. The growing applications of click chemistry. Chem Soc Rev 2007;36:1249–62. https://doi.org/10.1039/B613014N.

[42] Scrima M, Le Chevalier-Isaad A, Rovero P, Papini AM, Chorev M, D'Ursi AM. Cui catalyzed azide-alkyne intramolecular i-to-(i+4) side-chain-to-SideChain cyclization promotes the formation of Helix-like secondary structures. European J Org Chem 2010;2010:446–57. https://doi.org/10.1002/ejoc.200901157.

[43] Kawamoto SA, Coleska A, Ran X, Yi H, Yang CY, Wang S. Design of triazole-stapled BCL9 α-helical peptides to target the β-catenin/B-cell CLL/lymphoma 9 (BCL9) protein-protein interaction. J Med Chem 2012;55:1137–46. https://doi.org/10.1021/jm201125d.

[44] Madden MM, Muppidi A, Li Z, Li X, Chen J, Lin Q. Synthesis of cell-permeable stapled peptide dual inhibitors of the p53-Mdm2/Mdmx interactions via photoinduced cycloaddition. Bioorg Med Chem Lett 2011;21:1472–5. https://doi.org/10.1016/j.bmcl.2011.01.004.

[45] Jackson DY, King DS, Chmielewski J, Singh S, Schultz PG. General approach to the synthesis of short .alpha.-helical peptides. J Am Chem Soc 1991;113:9391–2. https://doi.org/10.1021/ja00024a067.

[46] Haney CM, Loch MT, Horne WS. Promoting peptide α-helix formation with dynamic covalent oxime side-chain cross-links. Chem Commun 2011;47:10915. https://doi.org/10.1039/c1cc12010g.

[47] Phelan JC, Skelton NJ, Braisted AC, McDowell RS. A general method for constraining short peptides to an α-helical conformation. J Am Chem Soc 1997;119:455–60. https://doi.org/10.1021/ja9611654.

[48] Spokoyny AM, Zou Y, Ling JJ, Yu H, Lin Y-S, Pentelute BL. A Perfluoroaryl-cysteine S_NAr chemistry approach to unprotected peptide stapling. J Am Chem Soc 2013;135:5946–9. https://doi.org/10.1021/ja400119t.

[49] Brunel FM, Dawson PE. Synthesis of constrained helical peptides by thioether ligation: application to analogs of gp41. Chem Commun 2005:2552–4. https://doi.org/10.1039/b419015g.

[50] Brunel FM, Zwick MB, Cardoso RMF, Nelson JD, Wilson IA, Burton DR, et al. Structure-function analysis of the epitope for 4E10, a broadly neutralizing human immunodeficiency virus type 1 antibody. J Virol 2006;80:1680. https://doi.org/10.1128/JVI.80.4.1680-1687.2006.

[51] RCSB. Protein data-bank. n.d www.rcsb.org.

[52] Briggs LC, Chan AWE, Davis CA, Whitelock N, Hotiana HA, Baratchian M, et al. IKKγ-mimetic peptides block the resistance to apoptosis associated with Kaposi's sarcoma-associated herpesvirus infection. J Virol 2017;91. https://doi.org/10.1128/JVI.01170-17 e01170–17.

[53] Rennie YK, McIntyre PJ, Akindele T, Bayliss R, Jamieson AG. A TPX2 Proteomimetic has enhanced affinity for Aurora-a due to hydrocarbon stapling of a Helix. ACS Chem Biol 2016;11:3383–90. https://doi.org/10.1021/acschembio.6b00727.

[54] Phillips NB, Wan ZL, Whittaker L, Hu SQ, Huang K, Hua QX, et al. Supramolecular protein engineering: design of zinc-stapled insulin hexamers as a long acting depot. J Biol Chem 2010;285:11755–9. https://doi.org/10.1074/jbc.C110.105825.

[55] Xu W, Lau YH, Fischer G, Tan YS, Chattopadhyay A, De La Roche M, et al. Macrocyclized extended peptides: inhibiting the substrate-recognition domain of Tankyrase. J Am Chem Soc 2017;139:2245–56. https://doi.org/10.1021/jacs.6b10234.

[56] Gunzburg MJ, Kulkarni K, Watson GM, Ambaye ND, Del Borgo MP, Brandt R, et al. Unexpected involvement of staple leads to redesign of selective bicyclic peptide inhibitor of Grb7. Sci Rep 2016;6:27060. https://doi.org/10.1038/srep27060.

[57] Ultsch M, Braisted A, Maun HR, Eigenbrot C. 3-2-1: structural insights from stepwise shrinkage of a three-helix fc-binding domain to a single helix. Protein Eng Des Sel 2017;30:619–25. https://doi.org/10.1093/protein/gzx029.
[58] Lama D, Quah ST, Verma CS, Lakshminarayanan R, Beuerman RW, Lane DP, et al. Rational optimization of conformational effects induced by hydrocarbon staples in peptides and their binding interfaces. Sci Rep 2013;3:3451. https://doi.org/10.1038/srep03451.
[59] McGrath S, Tortorici M, Drouin L, Solanki S, Vidler L, Westwood I, et al. Structure-enabled discovery of a stapled peptide inhibitor to target the oncogenic transcriptional repressor TLE1. Chem A Eur J 2017;23:9577–84. https://doi.org/10.1002/chem.201700747.
[60] Stelzl U, Worm U, Lalowski M, Haenig C, Brembeck FH, Goehler H, et al. A human protein-protein interaction network: a resource for annotating the proteome. Cell 2005;122:957–68. https://doi.org/10.1016/j.cell.2005.08.029.
[61] Kussie PH, Gorina S, Marechal V, Elenbaas B, Moreau J, Levine AJ, et al. Structure of the MSM2 oncoprotein bound to the p53 tumor suppressor transactivation domain. Science 1996;274 80-. (948–53).
[62] Baek S, Kutchukian PS, Verdine GL, Huber R, Holak TA, Lee KW, et al. Structure of the stapled p53 peptide bound to Mdm2. J Am Chem Soc 2012;134:103–6. https://doi.org/10.1021/ja2090367.
[63] Chee SMQ, Wongsantichon J, Soo Tng Q, Robinson R, Joseph TL, Verma C, et al. Structure of a stapled peptide antagonist bound to nutlin-resistant Mdm2. PLoS One 2014;9:e104914. https://doi.org/10.1371/journal.pone.0104914.
[64] Lau YH, Wu Y, Rossmann M, Tan BX, De Andrade P, Tan YS, et al. Double strain-promoted macrocyclization for the rapid selection of cell-active stapled peptides. Angew Chem Int Ed 2015;54:15410–3. https://doi.org/10.1002/anie.201508416.
[65] Tan YS, Reeks J, Brown CJ, Thean D, Ferrer Gago FJ, Yuen TY, et al. Benzene probes in molecular dynamics simulations reveal novel binding sites for ligand design. J Phys Chem Lett 2016;7:3452–7. https://doi.org/10.1021/acs.jpclett.6b01525.
[66] Chee SMQ, Wongsantichon J, Siau J, Thean D, Ferrer F, Robinson RC, et al. Structure-activity studies of Mdm2/Mdm4- binding stapled peptides comprising non- natural amino acids. PLoS One 2017;12:e0189379. https://doi.org/10.1371/journal.pone.0189379.
[67] Li X, Lu W. No title. To Be Published 2018.
[68] Stewart ML, Fire E, Keating AE, Walensky LD. The MCL-1 BH3 helix is an exclusive MCL-1 inhibitor and apoptosis sensitizer. Nat Chem Biol 2010;6:595–601. https://doi.org/10.1038/nchembio.391.
[69] Miles JA, Yeo DJ, Rowell P, Rodriguez-Marin S, Pask CM, Warriner SL, et al. Hydrocarbon constrained peptides-understanding preorganisation and binding affinity. Chem Sci 2016;7:3694–702. https://doi.org/10.1039/c5sc04048e.
[70] Rezaei Araghi R, Bird GH, Ryan JA, Jenson JM, Godes M, Pritz JR, et al. Iterative optimization yields mcl-1–targeting stapled peptides with selective cytotoxicity to mcl-1–dependent cancer cells. Proc Natl Acad Sci 2018;201712952. https://doi.org/10.1073/pnas.1712952115.
[71] Harvey EP, Seo HS, Guerra RM, Bird GH, Dhe-Paganon S, Walensky LD. Crystal structures of anti-apoptotic BFL-1 and Its complex with a covalent stapled peptide inhibitor. Structure 2018;26:153–60 e4 https://doi.org/10.1016/j.str.2017.11.016.
[72] Phillips C, Roberts LR, Schade M, Bazin R, Bent A, Davies NL, et al. Design and structure of stapled peptides binding to estrogen receptors. J Am Chem Soc 2011;133:9696–9. https://doi.org/10.1021/ja202946k.
[73] Speltz TE, Fanning SW, Mayne CG, Fowler C, Tajkhorshid E, Greene GL, et al. Stapled peptides with γ-methylated hydrocarbon chains for the estrogen receptor/coactivator interaction. Angew Chem Int Ed Engl 2016;55:4252–5. https://doi.org/10.1002/anie.201510557.
[74] Speltz TE, Mayne CG, Fanning SW, Siddiqui Z, Tajkhorshid E, Greene GL, et al. A "cross-stitched" peptide with improved helicity and proteolytic stability. Org Biomol Chem 2018;16:3702–6. https://doi.org/10.1039/c8ob00790j.
[75] Frank AO, Vangamudi B, Feldkamp MD, Souza-Fagundes EM, Luzwick JW, Cortez D, et al. Discovery of a potent stapled helix peptide that binds to the 70N domain of replication protein a. J Med Chem 2014;57:2455–61. https://doi.org/10.1021/jm401730y.
[76] Grossmann TN, Yeh JT-H, Bowman BR, Chu Q, Moellering RE, Verdine GL. Inhibition of oncogenic Wnt signaling through direct targeting of -catenin. Proc Natl Acad Sci 2012;109:17942–7. https://doi.org/10.1073/pnas.1208396109.
[77] Scott DC, Monda JK, Bennett EJ, Harper JW, Schulman BA. N-terminal acetylation acts as an avidity enhancer within an interconnected multiprotein complex. Science 2011;334. https://doi.org/10.1126/science.1209307 80-. 674–8.
[78] Findeisen F, Campiglio M, Jo H, Abderemane-Ali F, Rumpf CH, Pope L, et al. Stapled voltage-gated Calcium Channel (CaV) α-interaction domain (AID) peptides act as selective protein-protein interaction inhibitors of CaVFunction. ACS Chem Nerosci 2017;8:1313–26. https://doi.org/10.1021/acschemneuro.6b00454.
[79] Lee Y, Yoon H, Hwang SM, Shin MK, Lee JH, Oh M, et al. Targeted inhibition of the NCOA1/STAT6 protein-protein interaction. J Am Chem Soc 2017;139:16056–9. https://doi.org/10.1021/jacs.7b08972.
[80] Wu Y, Villa F, Maman J, Lau YH, Dobnikar L, Simon AC, et al. Targeting the genome-stability hub Ctf4 by stapled-peptide design. Angew Chem Int Ed 2017;56:12866–72. https://doi.org/10.1002/anie.201705611.
[81] Haney CM, Horne WS. Oxime side-chain cross-links in an α-helical coiled-coil protein: structure, thermodynamics, and folding-templated synthesis of bicyclic species. Chem A Eur J 2013;19:11342–51. https://doi.org/10.1002/chem.201300506.
[82] Tan WL, Wong KH, Lei J, Sakai N, Tan HW, Hilgenfeld R, et al. Lybatides from Lycium barbarum contain an unusual cystine-stapled helical peptide scaffold. Sci Rep 2017;7:1–11. https://doi.org/10.1038/s41598-017-05037-1.
[83] Jaskólski M, Wlodawer A, Tomasselli AG, Sawyer TK, Staples DG, Heinrikson RL, et al. Structure at 2.5-Å resolution of chemically synthesized human immunodeficiency virus type 1 protease complexed with a hydroxyethylene-based inhibitor. Biochemistry 1991;30:1600–9. https://doi.org/10.1021/bi00220a023.
[84] Swain AL, Miller MM, Green J, Rich DH, Schneider J, Kent SB, et al. X-ray crystallographic structure of a complex between a synthetic protease of human immunodeficiency virus 1 and a substrate-based hydroxyethylamine inhibitor. Proc Natl Acad Sci U S A 1990;87 (8805–9. doi:2247451).
[85] Bhattacharya S, Zhang H, Debnath AK, Cowburn D. Solution structure of a hydrocarbon stapled peptide inhibitor in complex with monomeric C-terminal domain of HIV-1 capsid. J Biol Chem 2008;283:16274–8. https://doi.org/10.1074/jbc.C800048200.
[86] Staple DW, Venditti V, Niccolai N, Elson-Schwab L, Tor Y, Butcher SE. Guanidinoneomycin B recognition of an HIV-1 RNA helix. ChemBioChem 2008;9:93–102. https://doi.org/10.1002/cbic.200700251.
[87] Staple DW, Butcher SE. Solution structure and thermodynamic investigation of the HIV-1 frameshift inducing element. J Mol Biol 2005;349:1011–23. https://doi.org/10.1016/j.jmb.2005.03.038.
[88] Staple DW, Butcher SE. Solution structure of the HIV-1 frameshift inducing stem-loop RNA. Nucleic Acids Res 2003;31:4326–31. https://doi.org/10.1093/nar/gkg654.
[89] Singh PK, Solanki V, Sharma S, Thakur KG, Krishnan B, Korpole S. The intramolecular disulfide-stapled structure of laterosporulin, a class IId bacteriocin, conceals a human defensin-like structural module. FEBS J 2015;282:203–14. https://doi.org/10.1111/febs.13129.
[90] Douse CH, Maas SJ, Thomas JC, Garnett JA, Sun Y, Cota E, et al. Crystal structures of stapled and hydrogen bond surrogate peptides targeting a fully buried protein-helix interaction. ACS Chem Biol 2014;9:2204–9. https://doi.org/10.1021/cb500271c.
[91] Aydin H, Cook JD, Lee JE. Crystal structures of Beta- and Gammaretrovirus fusion proteins reveal a role for electrostatic stapling in viral entry. J Virol 2014;88:143–53. https://doi.org/10.1128/JVI.02023-13.
[92] Lilic M, Galkin VE, Orlova A, VanLoock MS, Egelman EH, Stebbins CE. Actin by stapling filaments with nonglobular protein arms. Science 2003;301 80-. (1918–21).
[93] Byrne C, McEwan PA, Emsley J, Fischer PM, Chan WC. End-stapled homo and hetero collagen triple helices: a click chemistry approach. Chem Commun 2011;47:2589–91. https://doi.org/10.1039/c0cc04795c.
[94] Mercurio FA, Pirone L, Di Natale C, Marasco D, Pedone EM, Leone M. Sam domain-based stapled peptides: structural analysis and interaction studies with the Sam domains from the EphA2 receptor and the lipid phosphatase Ship2. Bioorg Chem 2018;80:602–10. https://doi.org/10.1016/j.bioorg.2018.07.013.
[95] De Paola I, Pirone L, Palmieri M, Balasco N, Esposito L, Russo L, et al. Cullin3 - BTB interface:a novel target for stapled peptides. PLoS One 2015;10:1–21. https://doi.org/10.1371/journal.pone.0121149.
[96] Marcheschi RJ, Staple DW, Butcher SE. Programmed ribosomal frameshifting in SIV is induced by a highly structured RNA stem-loop. J Mol Biol 2007;373:652–63. https://doi.org/10.1016/j.jmb.2007.08.033.
[97] Barthe P, Roumestand C, Rochette S, Vita C. Synthesis and NMR solution structure of an α-helical hairpin stapled with two disulfide bridges. Protein Sci 2000;9:942–55. https://doi.org/10.1110/ps.9.5.942.
[98] Byrne A, Kier BL, Williams DV, Scian M, Andersen NH. Circular permutation of the Trp-cage: fold rescue upon addition of a hydrophobic staple. RSC Adv 2013;3:19824–9. https://doi.org/10.1039/c3ra43674h.
[99] Brown CJ, Quah ST, Jong J, Goh AM, Chiam PC, Khoo KH, et al. Stapled peptides with improved potency and specificity that activate p53. ACS Chem Biol 2013;8:506–12. https://doi.org/10.1021/cb3005148.
[100] Thean D, Ebo JS, Luxton T, Lee XC, Yuen TY, Ferrer FJ, et al. Enhancing specific disruption of intracellular protein complexes by hydrocarbon stapled peptides using lipid based delivery. Sci Rep 2017;7:1–11. https://doi.org/10.1038/s41598-017-01712-5.
[101] Souers AJ, Leverson JD, Boghaert ER, Ackler SL, Catron ND, Chen J, et al. ABT-199, a potent and selective BCL-2 inhibitor, achieves antitumor activity while sparing platelets. Nat Med 2013;19:202–8. https://doi.org/10.1038/nm.3048.
[102] Singh RR, Kim JE, Davuluri Y, Drakos E, Cho-Vega JH, Amin HM, et al. Hedgehog signaling pathway is activated in diffuse large B-cell lymphoma and contributes to tumor cell survival and proliferation. Leukemia 2010;24:1025–36. https://doi.org/10.1038/leu.2010.35.
[103] Vogler M, Dinsdale D, Dyer MJS, Cohen GM. ABT-199 selectively inhibits BCL2 but not BCL2L1 and efficiently induces apoptosis of chronic lymphocytic leukaemic cells but not platelets. Br J Haematol 2013;163:139–42. https://doi.org/10.1111/bjh.12457.
[104] Vandenberg CJ, Cory S. ABT-199, a new Bcl-2–specific BH3 mimetic, has in vivo efficacy against aggressive Myc-driven mouse lymphomas without provoking thrombocytopenia. Blood 2013;121:2285–8. https://doi.org/10.1182/blood-2013-01-475855.
[105] Zhang B, Gojo I, Fenton RG. Myeloid cell factor-1 is a critical survival factor for multiple myeloma. Blood 2002;99:1885–93. https://doi.org/10.1182/blood.V99.6.1885.
[106] Konopleva M, Contractor R, Tsao T, Samudio I, Ruvolo PP, Kitada S, et al. Mechanisms of apoptosis sensitivity and resistance to the BH3 mimetic ABT-737 in acute myeloid leukemia. Cancer Cell 2006;10:375–88. https://doi.org/10.1016/j.ccr.2006.10.006.
[107] Boisvert-Adamo K, Longmate W, Abel EV, Aplin AE. Mcl-1 is required for melanoma cell resistance to Anoikis. Mol Cancer Res 2009;7:549–56. https://doi.org/10.1158/1541-7786.MCR-08-0358.
[108] Ding Q, He X, Xia W, Hsu JM, Te Chen C, Li LY, et al. Myeloid cell leukemia-1 inversely correlates with glycogen synthase kinase-3β activity and associates with

poor prognosis in human breast cancer. Cancer Res 2007;67:4564–71. https://doi.org/10.1158/0008-5472.CAN-06-1788.
[109] Heldring N, Pike A, Andersson S, Matthews J, Cheng G, Hartman J, et al. Estrogen receptors: how do they signal and what are their targets. Physiol Rev 2007;87:905–31. https://doi.org/10.1152/physrev.00026.2006.
[110] Clarke M. Meta-analyses of adjuvant therapies for women with early breast cancer: the early breast Cancer Trialists' collaborative group overview. Ann Oncol 2006;17:x59–62. https://doi.org/10.1093/annonc/mdl238.
[111] Abe O, Abe R, Enomoto K, Kikuchi K, Koyama H, Masuda H, et al. Effects of chemotherapy and hormonal therapy for early breast cancer on recurrence and 15-year survival: an overview of the randomised trials. Lancet 2005;365:1687–717. https://doi.org/10.1016/S0140-6736(05)66544-0.
[112] Tan YS, Lane DP, Verma CS. Stapled peptide design: principles and roles of computation. Drug Discov Today 2016;21:1642–53. https://doi.org/10.1016/j.drudis.2016.06.012.
[113] Cornillie SP, Bruno BJ, Lim CS, Cheatham TE. Computational modeling of stapled peptides toward a treatment strategy for CML and broader implications in the design of lengthy peptide therapeutics. J Phys Chem B 2018;122:3864–75. https://doi.org/10.1021/acs.jpcb.8b01014.
[114] Pettersen EF, Goddard TD, Huang CC, Couch GS, Greenblatt DM, Meng EC, et al. UCSF chimera - a visualization system for exploratory research and analysis. J Comput Chem 2004;25:1605–12. https://doi.org/10.1002/jcc.20084.
[115] Cornell WD, Cieplak P, Bayly CI, Gould IR, Kenneth M, Merz J, et al. A second generation force field for the simulation of proteins, nucleic acids, and organic molecules. J Am Chem Soc 1995;117:5179–97. https://doi.org/10.1021/ja00124a002.
[116] Hopkins CW, Le Grand S, Walker RC, Roitberg AE. Long-time-step molecular dynamics through hydrogen mass repartitioning. J Chem Theory Comput 2015;11:1864–74. https://doi.org/10.1021/ct5010406.
[117] Oltersdorf T, Elmore SW, Shoemaker AR, Armstrong RC, Augeri DJ, Belli BA, et al. An inhibitor of Bcl-2 family proteins induces regression of solid tumours. Nature 2005;435:677–81. https://doi.org/10.1038/nature03579.
[118] Vu BT, Vassilev L. Small-molecule inhibitors of the p53-MDM2 interaction. Curr Top Microbiol Immunol 2011;348:151–72. https://doi.org/10.1007/82_2010_110.
[119] Maloney A, Workman P. HSP90 as a new therapeutic target for cancer therapy: the story unfolds. Expert Opin Biol Ther 2002;2:3–24. https://doi.org/10.1517/14712598.2.1.3.
[120] Neckers L, Workman P. Hsp90 molecular chaperone inhibitors: are we there yet? Clin Cancer Res 2012;18:64–76. https://doi.org/10.1158/1078-0432.CCR-11-1000.
[121] Trudel S, Zhi HL, Rauw J, Tiedemann RE, Xiao YW, Stewart AK. Preclinical studies of the pan-Bcl inhibitor obatoclax (GX015-070) in multiple myeloma. Blood 2007;109:5430–8. https://doi.org/10.1182/blood-2006-10-047951.
[122] Nguyen M, Marcellus RC, Roulston A, Watson M, Serfass L, Murthy Madiraju SR, et al. Small molecule obatoclax (GX15-070) antagonizes MCL-1 and overcomes MCL-1-mediated resistance to apoptosis. Proc Natl Acad Sci 2007;104:19512–7. https://doi.org/10.1073/pnas.0709443104.
[123] Paik PK, Rudin CM, Pietanza MC, Brown A, Rizvi NA, Takebe N, et al. A phase II study of obatoclax mesylate, a Bcl-2 antagonist, plus topotecan in relapsed small cell lung cancer. Lung Cancer 2011;74:481–5. https://doi.org/10.1016/j.lungcan.2011.05.005.
[124] Billard C. Design of novel BH3 mimetics for the treatment of chronic lymphocytic leukemia. Leukemia 2012;26:2032–8. https://doi.org/10.1038/leu.2012.88.
[125] Vassilev LT, Vu BT, Graves B, Carvajal D, Podlaski F, Filipovic Z, et al. In vivo activation of the p53 pathway by small-molecule antagonists of MDM2. Science 2004;303. https://doi.org/10.1126/science.1092472 80-. 844–8.
[126] Schulte TW, Neckers LM. The benzoquinone ansamycin 17-allylamino-17-demethoxygeldanamycin binds to HSP90 and shares important biologic activities with geldanamycin. Cancer Chemother Pharmacol 1998;42:273–9. https://doi.org/10.1007/s002800050817.
[127] Bird GH, Mazzola E, Opoku-Nsiah K, Lammert MA, Godes M, Neuberg DS, et al. Biophysical determinants for cellular uptake of hydrocarbon-stapled peptide helices. Nat Chem Biol 2016. https://doi.org/10.1038/nchembio.2153.
[128] Lalatsa A, Schatzlein AG, Uchegbu IF. Strategies to deliver peptide drugs to the brain. Mol Pharm 2014;11:1081–93. https://doi.org/10.1021/mp400680d.
[129] Melmed S, Popovic V, Bidlingmaier M, Mercado M, van der Lely AJ, Biermasz N, et al. Safety and efficacy of Oral octreotide in acromegaly: results of a multicenter phase III trial. J Clin Endocrinol Metab 2015;100:1699–708. https://doi.org/10.1210/jc.2014-4113.
[130] Brayden DJ, Alonso M-J. Oral delivery of peptides: opportunities and issues for translation. Adv Drug Deliv Rev 2016;106:193–5. https://doi.org/10.1016/J.ADDR.2016.10.005.
[131] Wallbrecher R, Chène P, Ruetz S, Stachyra T, Vorherr T, Brock R. A critical assessment of the synthesis and biological activity of p53/human double minute 2-stapled peptide inhibitors. Br J Pharmacol 2017;174:2613–22. https://doi.org/10.1111/bph.13834.
[132] Okamoto T, Zobel K, Fedorova A, Quan C, Yang H, Fairbrother WJ, et al. Stabilizing the pro-apoptotic BimBH3 helix (BimSAHB) does not necessarily enhance affinity or biological activity. ACS Chem Biol 2013;8:297–302. https://doi.org/10.1021/cb3005403.
[133] Moellering RE, Cornejo M, Davis TN, Del Bianco C, Aster JC, Blacklow SC, et al. Direct inhibition of the NOTCH transcription factor complex. Nature 2009;462:182–8. https://doi.org/10.1038/nature08543.
[134] Weng Z, Zhao Q. Utilizing ELISA to monitor protein-protein interaction. Protein-protein interact. Methods appl2nd ed. ; 2015. https://doi.org/10.1007/978-1-4939-2425-7_21 p. 341–52.
[135] Mattheyses AL, Marcus AI. Förster resonance energy transfer (FRET) microscopy for monitoring biomolecular interactions. Protein-protein interact. Methods appl2nd ed. ; 2015. https://doi.org/10.1007/978-1-4939-2425-7_20 p. 329–39.
[136] Bacart J, Corbel C, Jockers R, Bach S, Couturier C. The BRET technology and its application to screening assays. Biotechnol J 2008;3:311–24. https://doi.org/10.1002/biot.200700222.
[137] Söderberg O, Gullberg M, Jarvius M, Ridderstråle K, Leuchowius KJ, Jarvius J, et al. Direct observation of individual endogenous protein complexes in situ by proximity ligation. Nat Methods 2006;3:995–1000. https://doi.org/10.1038/nmeth947.
[138] Bernal F, Wade M, Godes M, Davis TN, Whitehead DG, Kung AL, et al. A stapled p53 Helix overcomes HDMX-mediated suppression of p53. Cancer Cell 2010;18:411–22. https://doi.org/10.1016/j.ccr.2010.10.024.
[139] Herce HD, Deng W, Helma J, Leonhardt H, Cardoso MC. Visualization and targeted disruption of protein interactions in living cells. Nat Commun 2013;4. https://doi.org/10.1038/ncomms3660.
[140] Li Y, Rodewald LW, Hoppmann C, Wong ET. A versatile platform to analyze low affinity and transient protein- protein interactions in living cells in real time, vol. 9; 2014; 1946–58. https://doi.org/10.1016/j.celrep.2014.10.058.A.